SULPHUR

The Eh-pH diagram for sulfur species in the water stability field is shown in Fig. 3. The thermodynamic data for important naturally occurring sulfur species are given in Table 3.

The sulfur Eh-pH diagram presented here is calculated on the basis of an assumed activity of dissolved sulfur = 10^{-3}, since this is a reasonable value for many terrestrial waters. Garrels and Christ (1965) and others have presented sulfur Eh-pH diagrams for both much greater and lower activities of dissolved sulfur. For an increase in the activity of dissolved S, the field of native sulfur increases, and for a decrease in the S activity, it decreases and disappears at about 10^{-6}.

Sulfur is an important element in the terrestrial systeme. Here, I have chosen to include only those species of major importance, and not those species of short, metastable existence. Thus, sulfites and thiosulfites and other anionic sulfur species are not given here. The diagrams for various metals with sulfur in the form of metal sulfides are given under the heading of each metallic element later in this book.

The boundary between (S(−II) and S(VI) is one of the most important in terrestrial systems. The oxidation of S(−II) species to S(VI) species is very energetic, and important for a wide variety of changes in mineral assemblages. These will be commented on under the various metallic element headings.

The thermodynamic data are all taken from Wagman et al. (1982) and are internally consistent.

Table 3. Thermodynamic data for sulfur

Species (state)	ΔG_f^0 (kcal/gfw)	Reference
S^{2-} (aq)	+20.51	Wagman et al. (1982)
HS^- (aq)	+2.89	Wagman et al. (1982)
H_2S (aq)	−6.65	Wagman et al. (1982)
SO_3^{2-} (aq)	−116.28	Wagman et al. (1982)
HSO_3^- (aq)	−126.13	Wagman et al. (1982)
SO_4^{2-} (aq)	−177.95	Wagman et al. (1982)
HSO_4^- (aq)	−180.67	Wagman et al. (1982)

Abbreviations see Table 1

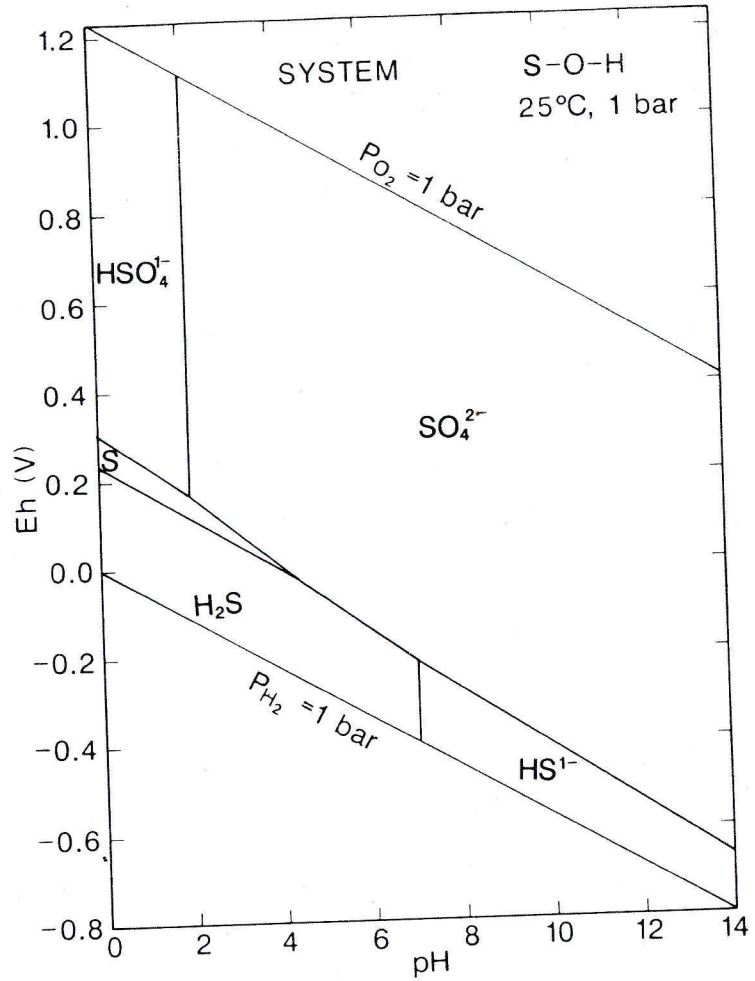

Fig. 3. Eh-pH diagram for part of the system S-O-H.
The activity of dissolved S = 10^{-3} (roughly 32 ppm) for convenience. The importance the boundary between sulfate (HSO_4^-, SO_4^{2-}) and sulfide (H_2S, HS^-, S^{2-}), exclusive native S, is discussed in the text

SELENIUM

The Eh-pH diagram for selenium species is shown in Fig. 4. The thermodynamic data for important naturally occurring selenium species are given in Table 4.

The Eh-pH diagram presented here is calculated on the basis of an assumed activity of dissolved selenium of 10^{-6}. Selenium is a rare element in the earth's crust, but one of considerable environmental interest due to its ready incorporation into the food chain. While excess selenium can cause adverse health effects, so, too, can extreme selenium deficiency. The Eh-pH diagram is marked by large stability fields of native selenium, $HSeO_3^-$, SeO_3^{2-}, and SeO_4^{2-}. The selenite species are especially important as they have been linked to adverse health effects. The field of native Se will increase with increased Se activity, and diminish with decreased Se activity.

Selenium can often substitute for sulfur in nature, commonly as Se (−II) for S(−II) in sulfides, forming seleniferous pyrite and other Se-bearing sulfides. The Se analog for pyrite, ferroselite ($FeSe_2$) occurs rarely in nature. Howard (1977) has published an extensive review of the selenium Eh-pH systematics, and presented diagrams showing the stability field of $FeSe_2$. There is not good agreement on the ΔG_f^0 for ferroselite, however, and I have not included the species here. The reader is referred to Howard (1977) for details on this matter. Other selenium Eh-pH diagrams of interest are given in Brookins (1979) and Thomson et al. (1986).

Table 4. Thermodynamic data for selenium

Species (state)	ΔG_f^0 (kcal/gfw)	Reference
Se^{2-} (aq)	+30.90	Wagman et al. (1982)
HSe^- (aq)	+10.50	Wagman et al. (1982)
H_2Se (aq)	+3.80	Wagman et al. (1982)
H_2SeO_3 (aq)	−101.85	Wagman et al. (1982)
$HSeO_3^-$ (aq)	−98.34	Wagman et al. (1982)
SeO_3^{2-} (aq)	−88.38	Wagman et al. (1982)
$HSeO_4^-$ (aq)	−108.08	Wagman et al. (1982)
SeO_4^{2-} (aq)	−105.47	Wagman et al. (1982)

Abbreviations see Table 1

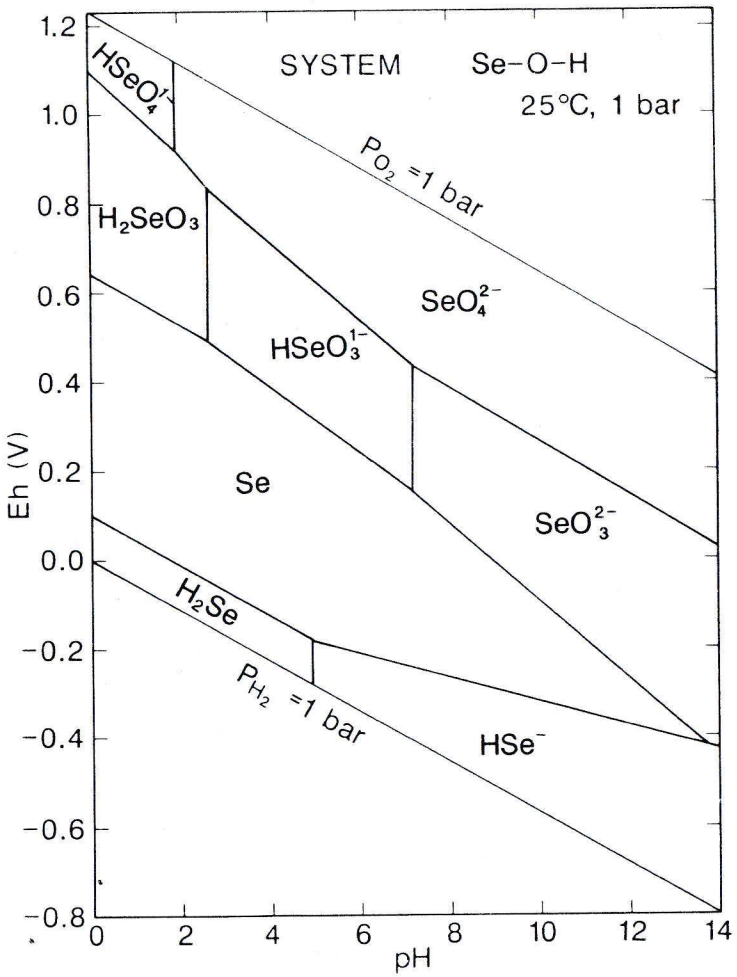

Fig. 4. Eh-pH diagram for part of the system Se-O-H. The activity of dissolved Se = 10^{-6}. See text for discussion

POLONIUM

The Eh-pH diagram for polonium species is shown in Fig. 6. The thermodynamic data for some important polonium species are given in Table 6.

Polonium isotopes are all radioactive, and ^{208}Po has the longest half-life of these at 2.9×10^3 years. In addition, ^{210}Po (half-life 138 days) is an intermediate decay product of ^{222}Rn (in turn from ^{238}U) and an is important potential carcinogen. Thus, polonium is of environmental importance.

The Eh-pH diagram (Fig. 6) shows a large field of native polonium, and a somewhat isolated field of PoS. PoO_2 is important under oxidizing conditions, especially at intermediate to basic pH, while a large field of Po^{2+} occupies most of the acidic, oxidizing Eh-pH space. The assumed activity of dissolved Po = 10^{-8} is reasonable based on the few polonium data available. A small field of Po^{4+} occurs under the most extreme acidic, oxidizing conditions.

Brookins (1978b, c) has published earlier versions of Fig. 6.

Table 6. Thermodynamic data for polonium

Species (state)	ΔG_f^0 (kcal/gfw)	Reference
Po^{2+} (aq)	+16.97	Wagman et al. (1982)
Po^{4+} (aq)	+70.00	Wagman et al. (1982)
$Po(OH)_4$ (c)	−130.00	Wagman et al. (1982)
$Po(OH)_2^{4+}$ (aq)	−113.05	Wagman et al. (1982)
PoS (c)	−0.96	Wagman et al. (1982)
PoO_2 (c)	−46.60	Latimer (1952)

Abbreviations see Table 1

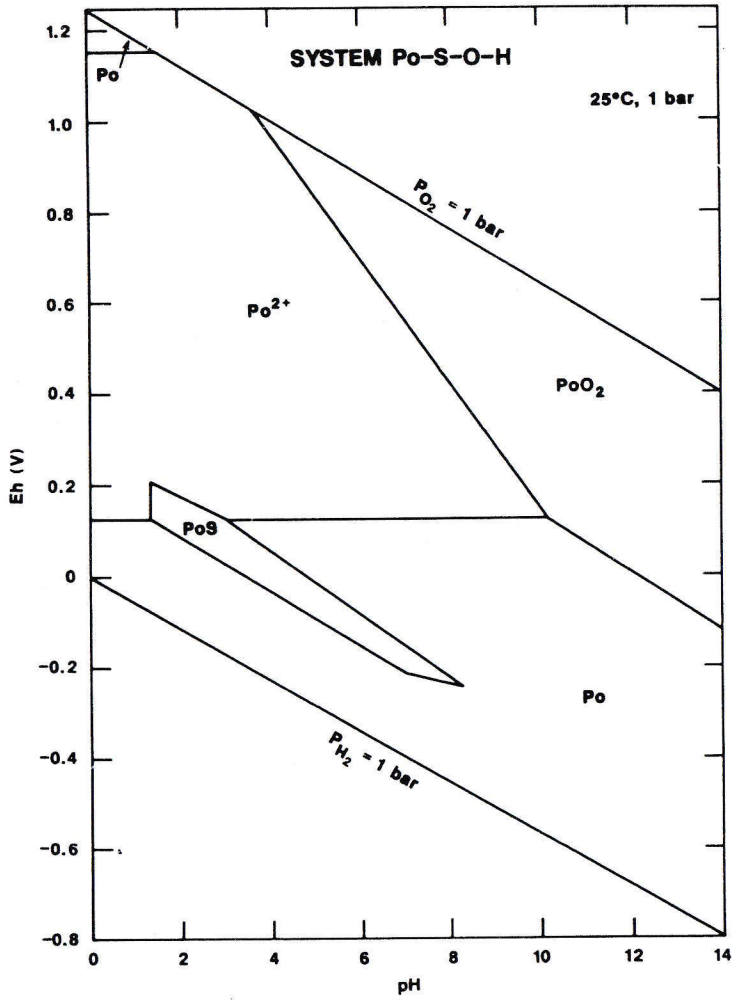

Fig. 6. Eh-pH diagram for part of the system Po-S-O-H. The assumed activities are: Po = 10^{-8}, S = 10^{-3}

NITROGEN

The Eh-pH diagram for nitrogen species is shown in Fig. 7. The thermodynamic data for important nitrogen species are given in Table 7.

Aqueous species of nitrogen in surface and groundwaters are dominated by nitrate ion under oxidizing conditions and ammonium ion under reducing conditions. If the waters are in communication with the atmosphere, then a large field of dissolved nitrogen gas occupies most of the Eh-pH space. For Fig. 7, the equilibrium condition of $P_{N_2} = 0.8$ atm ($= 10^{-3.3}$ activity) is assumed (Berner 1971). Under extreme basic, reducing conditions, a small field of ammonia gas appears.

Other nitrogen species, nitrites, nitriles, nitrous and nitric oxides, etc., are not considered here. In nature, a number of stable nitrates and ammonium compounds exist. These are not plotted in Fig. 7 because most nitrites are water soluble as are ammonium halide salts, and, for others, their thermodynamic data are not well known.

Table 7. Thermodynamic data for nitrogen

Species (state)	ΔG_f^0 (kcal/gfw)	Reference
N_2 (g)	0.00	Wagman et al. (1982)
NO_3^- (aq)	−25.99	Wagman et al. (1982)
NH_4^+ (aq)	−18.96	Wagman et al. (1982)
NH_3 (g)	−3.98	Berner (1971)

Abbreviations see Table 1

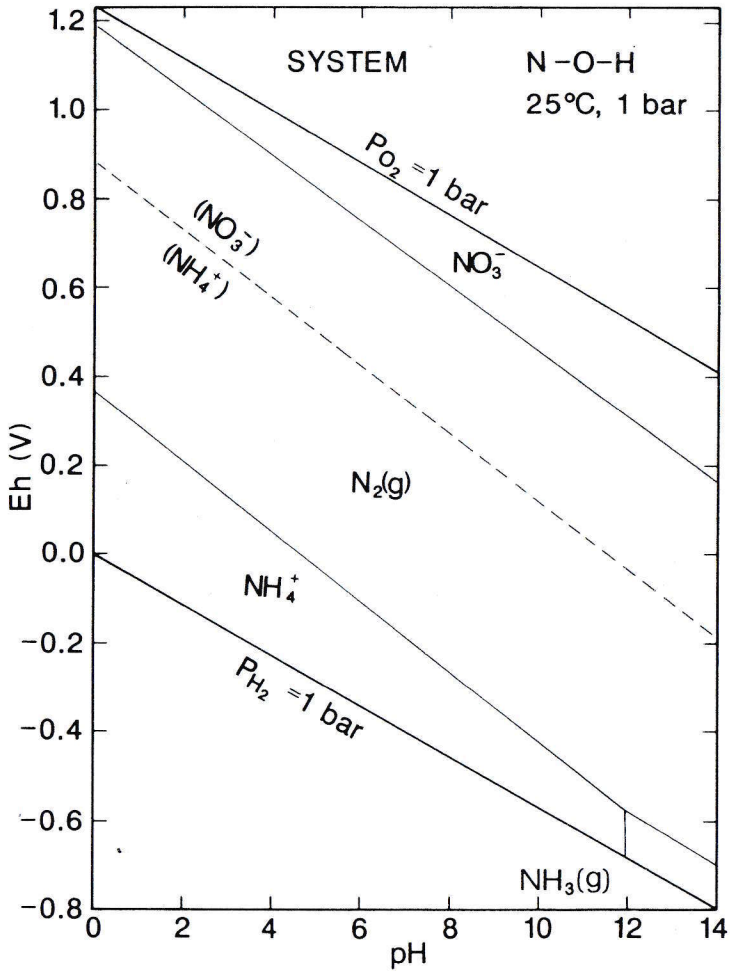

Fig. 7. Eh-pH diagram for part of the system N-O-H. The assumed activity of dissolved nitrogen = $10^{-3.3}$ ($P_{N_2} = 0.8$ bar). See text for discussion

ARSENIC

The Eh-pH diagrams for arsenic species are shown in Figs. 9 and 10. The thermodynamic data for important arsenic species are given in Table 9.

Figure 9 shows the Eh-pH relationships in the system As-O-H assuming an activity of 10^{-6} for dissolved arsenic. Dove and Rimstidt (1985) have also shown a similar diagram and, in a later figure, also included Fe as well to show the stability field of scorodite. In Fig. 9, however, only species in the simple As-O-H system are shown. A field of As_2O_3 is indicated by the dotted lines just above the field of native arsenic under mildly reducing, acidic conditions. Figure 9 is perhaps a bit misleading as it implies a moderate to fairly large field of native arsenic, and this occurrence is rare in nature. Figure 10, on the other hand, shows the effect of sulphur on the arsenic systematics. Here, it is noted that native arsenic occurs in the water stability field only under extremely basic, most reducing conditions. In Fig. 10, the fields of arsenous acid (H_3AsO_3) and its ionization products ($H_2AsO_3^-$, $HAsO_3^{2-}$, and AsO_3^{3-}) have been omitted for clarity in presentation. The field of As_2O_3 (either arsenolite or claudetite) occurs under acidic to neutral pH just above the sulfide-sulfate fence.

Both Figs. 9 and 10 indicate that arsenic acid and its ionization products are of prime importance for As transport under a very wide range of Eh and pH.

Arsenic in some minerals is present as As(−II), in which case it substitutes readily for S(−II). The oxygen fugacities for such minerals to form must be below the lower stability limit of water as the species H_2As and HAs^- plot well below the lower limit of water.

Table 9. Thermodynamic data for arsenic

Species (state)	ΔG_f^0 (kcal/gfw)	Reference
As (c)	0.00	Wagman et al. (1982)
AsS (c)	−16.80	Robie et al. (1978)
As_2S_3 (c)	−40.30	Wagman et al. (1982)
As_2O_3 (c)	−137.66	Robie et al. (1978)
H_3AsO_4 (aq)	−183.08	Wagman et al. (1982)
$H_2AsO_4^-$ (aq)	−180.01	Wagman et al. (1982)
$HAsO_4^{2-}$ (aq)	−170.69	Wagman et al. (1982)
AsO_4^{3-} (aq)	−154.97	Wagman et al. (1982)
H_3AsO_3 (aq)	−152.92	Wagman et al. (1982)
$H_2AsO_3^-$ (aq)	−140.33	Wagman et al. (1982)
$HAsO_3^{2-}$ (aq)	−125.31	Dove and Rimstidt (1985)
AsO_3^{3-} (aq)	−107.00	Dove and Rimstidt (1985)

Abbreviations see Table 1

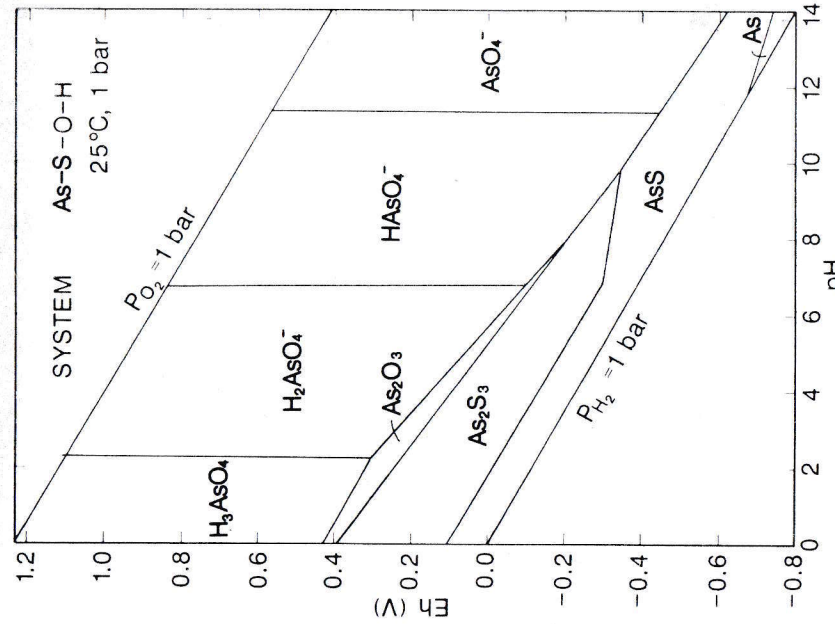

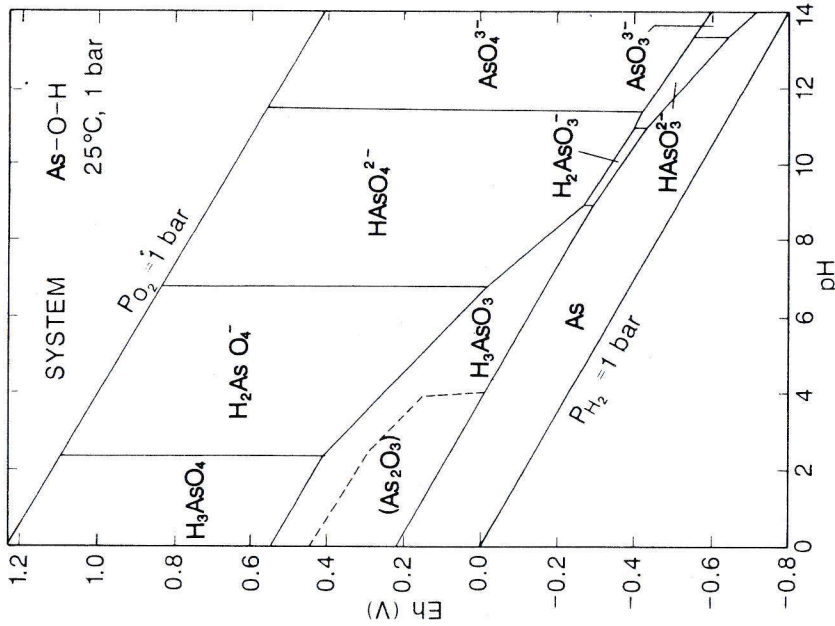

LEAD

The Eh-pH diagram for lead species is shown in Fig. 18. The thermodynamic data for important lead species are given in Table 16.

The Eh-pH diagram for part of the system Pb-S-C-O-H assumes activities of dissolved species as follows: Pb = 10^{-6}, S = 10^{-3}, C = 10^{-3}. Under reducing conditions, PbS (galena) occupies the Eh-pH space. Native Pb is metastable, as it falls below the lower stability limit of water under sulfur-present conditions. In the absence of sulfur, or at greatly reduced sulfur activity, native Pb is stable [i.e., the Pb : PbO boundary would intersect the Eh axis at 0.26 V with the slope parallel to the limits of the water stability field (−0.059 pH)]. When the sulfide-sulfate boundary is encountered, S(−II) is oxidized to S(VI) but Pb(II) remains unchanged. This results in a very small field of Pb^{2+} at pH below 0.4, followed (with increasing pH) by fields of $PbSO_4$ (anglesite), $PbCO_3$ (cerussite), and PbO (massicot or litharge). Under very oxidizing, near-neutral to basic pH, Pb(II) oxidizes to Pb(III) (i.e., in Pb_3O_4; minium) and Pb(IV) (i.e., PbO_2; plattnerite).

Under low dissolved C and S conditions, the field of Pb^{2+} is much larger. Lead is a very problematic element from environmental viewpoints. Tetraethyl lead from gasoline fumes causes buildup of Pb along roadways which enter the food chain; Pb in paint has been banned from use inside structures for health reasons.

Garrels and Christ (1965) and Brookins (1978b, c) have published Eh-pH diagrams for Pb species.

Table 16. Thermodynamic data for lead

Species (state)	ΔG_f^0 (kcal/gfw)	Reference
Pb^{2+} (aq)	−5.84	Wagman et al. (1982)
PbO (c, red)	−45.16	Wagman et al. (1982)
PbO_2 (c)	−51.94	Wagman et al. (1982)
Pb_3O_4 (c)	−143.69	Wagman et al. (1982)
$PbOH^+$ (aq)	−54.09	Wagman et al. (1982)
$HPbO_2^-$ (aq)	−80.88	Wagman et al. (1982)
PbS (c)	−23.59	Wagman et al. (1982)
$PbSO_4$ (c)	−194.35	Wagman et al. (1982)
$PbCO_3$ (c)	−149.50	Wagman et al. (1982)
$PbCl_3^-$ (aq)	−101.69	Wagman et al. (1982)

Abbreviations see Table 1

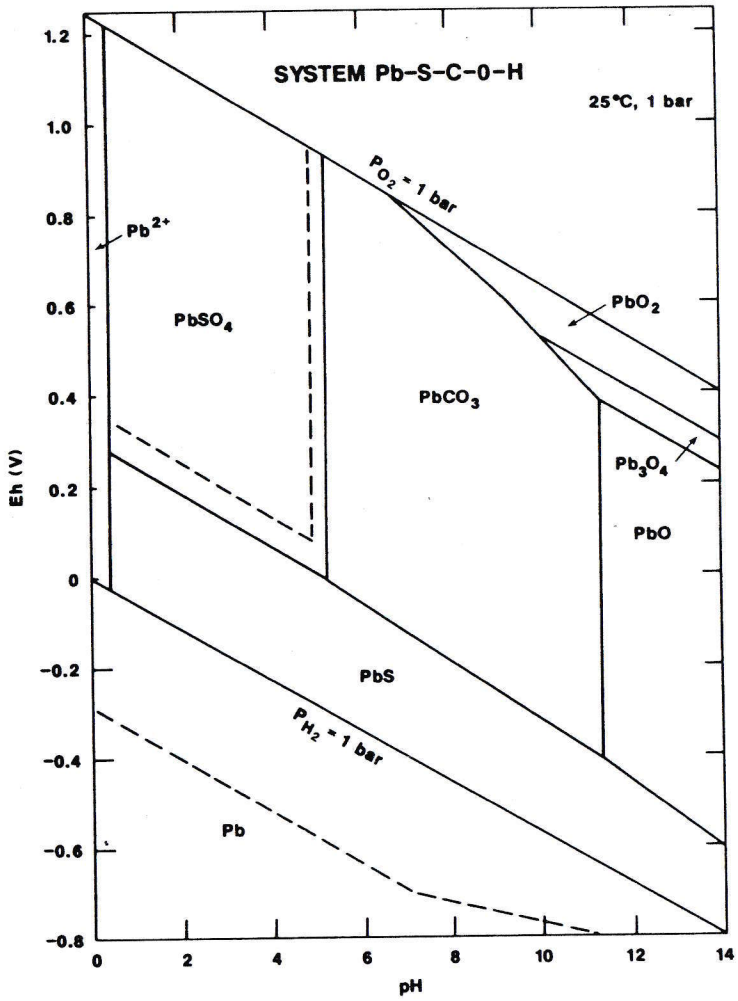

Fig. 18. Eh-pH diagram for part of the system Pb-S-C-O-H. The assumed activities of dissolved species are: Pb = $10^{-6,-8}$, S = 10^{-3}, C = 10^{-3}. See text for discussion

ALUMINUM

The Eh-pH diagram for aluminum species is shown in Fig. 20. The thermodynamic data for important aluminum species are given in Table 18.

Aluminum possess only one important valence, Al(III) in nature, and the insolubility of Al over much of the natural pH range is well known. In Fig. 20 the stability fields as a function of pH are plotted. Under acidic conditions, Al is soluble as Al^{3+} or $AlOH^{2+}$, although only Al^{3+} is shown for convenience. In the pH range, 3.7 – 11.3 solid $Al(OH)_3$ (gibbsite) is stable, assuming an activity of dissolved Al = 10^{-4}. Above pH 11.3, aqueous AlO_2^- occurs. For a lower activity, 10^{-6}, the pH range for $Al(OH)_3$ solid is 4.4 – 7.25.

Table 18. Thermodynamic data for aluminum

Species (state)	ΔG_f^0 (kcal/gfw)	Reference
Al^{3+} (aq)	−115.92	Wagman et al. (1982)
AlO_2^- (aq)	−198.59	Wagman et al. (1982)
$Al(OH)_3$ (gibbsite)	−276.08	Wagman et al. (1982)
$AlOH^{2+}$ (aq)	−165.89	Wagman et al. (1982)

Abbreviations see Table 1

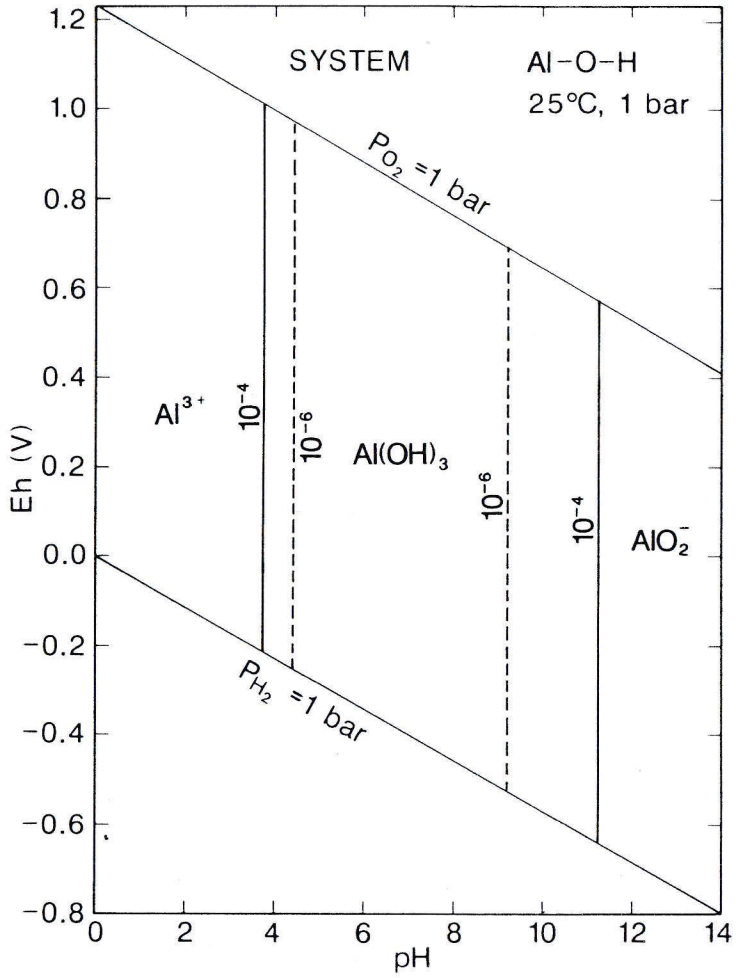

Fig. 20. Eh-pH diagram for part of the system Al-O-H. The assumed activity of dissolved Al = $10^{-4, -6}$. See text for discussion

ZINC

The Eh-pH diagram for zinc species is shown in Fig. 24. The thermodynamic data for important zinc species are given in Table 22.

Zinc possesses only one common valence Zn(II) in nature, yet zinc is dependent on redox conditions because of the stability of ZnS (sphalerite). In Fig. 24 the schematics of part of the system Zn-O-H-S-C are shown, and it is noted that under reducing conditions, below the sulfide-sulfate boundary, ZnS occupies much of the Eh-pH space. ZnS dissolves to Zn^{2+} at about pH 2.1 assuming an activity of dissolved zinc of 10^{-6} (pH = 1.14 for 10^{-4}). Above the sulfide-sulfate boundary, Zn^{2+} occupies a large Eh-pH field to pH = 7.5 ($a_{Zn} = 10^{-4}$), then a narrow field of $ZnCO_3$ (smithsonite), followed by a larger field of ZnO (zincite), which dissolves to form ZnO_2^{2-} at pH = 11 ($a_{Zn} = 10^{-8}$) or 13 ($a_{Zn} = 10^{-4}$).

Table 22. Thermodynamic data for zinc

Species (state)	ΔG_f^0 (kcal/gfw)	Reference
Zn^{2+} (aq)	−35.15	Wagman et al. (1982)
ZnO (c)	−76.08	Wagman et al. (1982)
ZnO_2^{2-} (aq)	−91.84	Wagman et al. (1982)
$ZnOH^+$ (aq)	−78.90	Wagman et al. (1982)
$HZnO_2^-$ (aq)	−109.42	Wagman et al. (1982)
$Zn(OH)_2$ (c)	−132.36	Wagman et al. (1982)
ZnS (c)	−48.11	Wagman et al. (1982)
$ZnCO_3$ (c)	−174.84	Wagman et al. (1982)

Abbreviations see Table 1

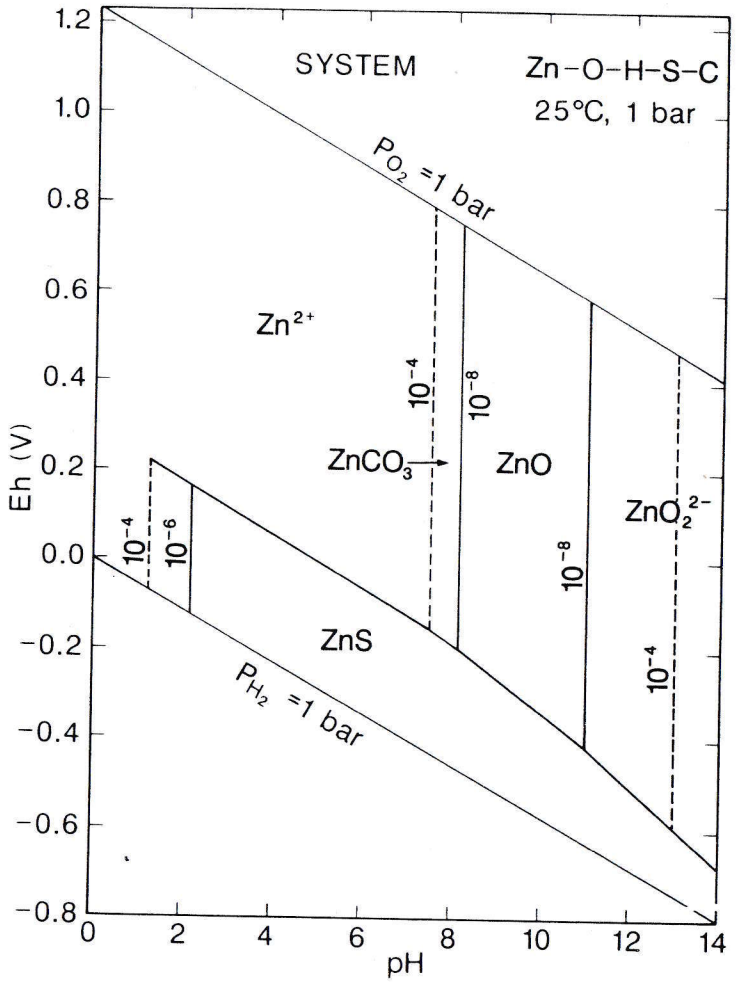

Fig. 24. Eh-pH diagram for part of the system Zn-O-H-S-C. The assumed activities for dissolved species are: Zn = $10^{-6, -4}$, C = 10^{-3}, S = 10^{-3}. See text for discussion

CADMIUM

The Eh-pH diagram for cadmium species is shown in Fig. 25. The thermodynamic data for important cadmium species are given in Table 23.

The Eh-pH diagram for the system Cd-C-S-O-H (Fig. 25) is fairly similar to that for the system Zn-O-H-S-C (Fig. 24) which is to be suspected based on their geochemical similarities. In Fig. 25, $a_{Cd} = 10^{-8}$ is assumed for all boundaries involving dissolved Cd. Below the sulfide-sulfate boundary, a large field of CdS (greenockite) exists, although in nature much of the Cd under these conditions is camouflaged by Zn in minerals such as sphalerite. Above this boundary, Cd^{2+} occupies a large Eh-pH field under slightly basic to very acidic pH. At higher pHs, $CdCO_3$ forms, then $Cd(OH)_2$, and then aqueous CdO_2^{2-}. Brookins (1986a) has published a preliminary Eh-pH diagram for Cd species for 25 °C, 1 bar; and he (Brookins 1979) has also calculated the 200 °C, 1 bar diagram in conjunction with studies of the Oklo Natural Reactor, Gabon.

Table 23. Thermodynamic data for cadmium

Species (state)	ΔG_f^0 (kcal/gfw)	Reference
Cd^{2+} (aq)	−18.55	Wagman et al. (1982)
$Cd(OH)_2$ (c)	−113.19	Wagman et al. (1982)
CdS (c)	−37.40	Wagman et al. (1982)
CdO_2^{2-} (aq)	−67.97	Wagman et al. (1982)
$CdCO_3$ (c)	−160.00	Wagman et al. (1982)
$CdSO_4$ (c)	−196.33	Wagman et al. (1982)
CdO (c)	−54.59	Wagman et al. (1982)

Abbreviations see Table 1

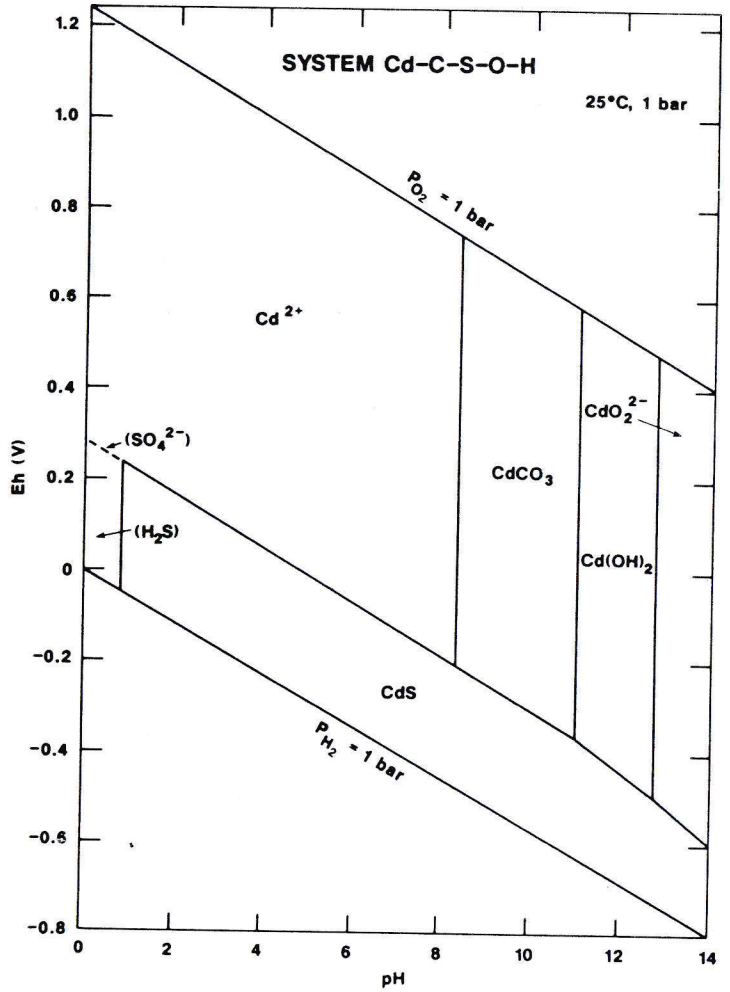

Fig. 25. Eh-pH diagram for part of the system Cd-C-S-O-H. The assumed activities for dissolved species are: Cd = 10^{-8}, C = 10^{-3}, S = 10^{-3}. See text for discussion

MERCURY

The Eh-pH diagram for mercury species is shown in Fig. 26. The thermodynamic data for important mercury species are given in Table 24.

Mercury species in the system Hg-S-O-H are shown by solid lines in Fig. 26. Dashed lines are used to show fields for $HgCl_4^{2-}$ and Hg_2Cl_2 (calomel), if Cl is added to the Hg-S-O-H system. In the absence of Cl, the oxidizing, acidic part of the Eh-pH diagram is occupied by mercurous ion Hg_2^{2-} and mercuric ion Hg^{2+}. Most of the Eh-pH diagram above the sulfide-sulfate boundary is occupied by a large field of native Hg. Montroydite (HgO) forms from native mercury at higher redox between pH = 5.4 to 10.6. Montroydite dissolves to form $HHgO_2^-$. For dissolved Hg with an activity of 10^{-9}, the fields of mercurous and mercuric ions are replaced by the chloride species of Hg as shown ($a_{Cl} = 10^{-3.5}$), showing the importance of Cl on mercury transport under oxidizing, acidic conditions.

Previous diagrams for the system Hg-O-H-S-Cl have been given by Parks and Nordström (1979).

Table 24. Thermodynamic data for mercury

Species (state)	ΔG_f^0 (kcal/gfw)	Reference
Hg_2^{2+} (aq)	+36.69	Wagman et al. (1982)
Hg^{2+} (aq)	+39.29	Wagman et al. (1982)
$HgOH^{1+}$ (aq)	−12.50	Wagman et al. (1982)
$HHgO_2^-$ (aq)	−45.48	Wagman et al. (1982)
HgS (c)	−12.09	Wagman et al. (1982)
HgS_2^{2-} (aq)	+41.90	Wagman et al. (1982)
HgO (c)	−58.56	Wagman et al. (1982)
Hg_2Cl_2 (c)	−50.38	Wagman et al. (1982)
$HgCl_4^{2-}$ (aq)	−106.79	Wagman et al. (1982)

Abbreviations see Table 1

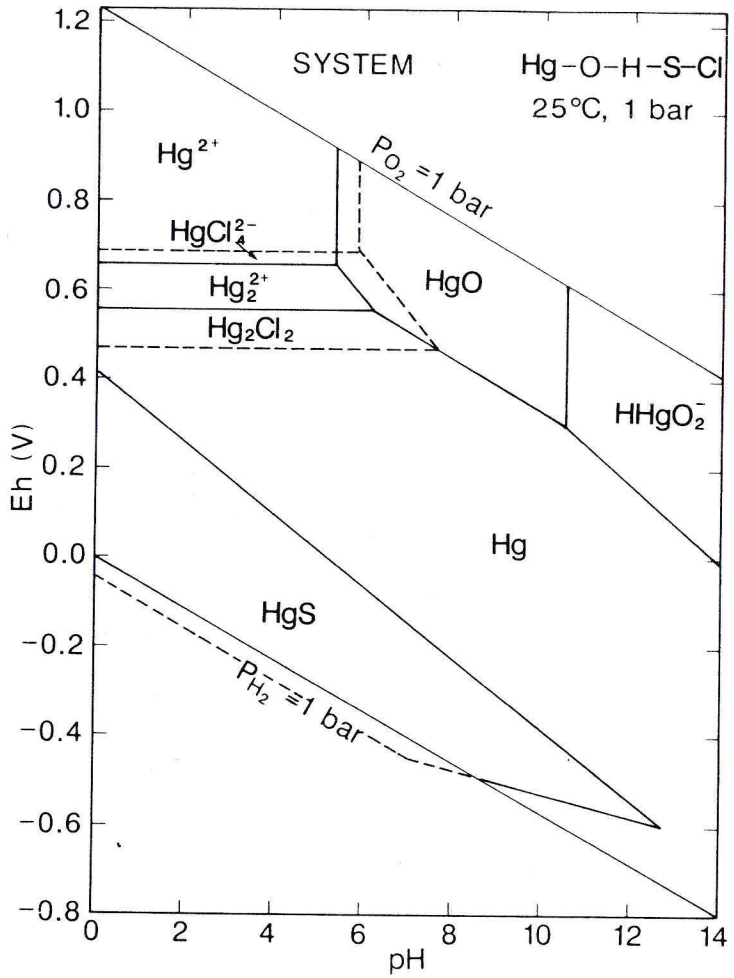

Fig. 26. Eh-pH diagram for part of the system Hg-O-H-S-Cl. The assumed activities for dissolved species are: Hg = 10^{-8}, Cl = $^{-3.5}$, S = 10^{-3}. See text for discussion

COPPER

Three Eh-pH diagrams for copper species are shown as Figs. 27–29. The thermodynamic data for important copper species are given in Table 25.

The simple system Cu-O-H Eh-pH diagram is shown in Fig. 27. An activity of dissolved Cu = 10^{-6} is assumed. The diagram is characterized by a large field of native copper under reducing conditions, but note that this field persits above the hypothetical sulfide-sulfate boundary (see Fig. 1). Native copper oxidizes to cupric ion, Cu^{2+}, under acidic pH, then to Cu_2O (cuprite). Cuprite, in turn, oxidizes to CuO (tenorite) under higher Eh conditions. At very high pH, CuO dissolves to form CuO_2^-, and cuprite oxidizes to this species as well.

In Fig. 28 the phase relations in the system Cu-S-O-H are shown. Here, two important sulfides appear below the sulfide-sulfate boundary. Chalcocite (Cu_2S) and covellite (CuS) both occupy significant parts of the Eh-pH diagram. Note, however, that above the sulfide-sulfate boundary, as sulfate forms from S(−II), Cu^{1+} from chalcocite is reduced to native copper. The relative fields of Cu_2O, CuO, CuO_2^{2-}, and most of the Cu^{2+} field are identical to those shown in Fig. 27.

Figure 29 shows the phase relations when C is added. Malachite is the most important cupric carbonate in the system Cu-C-S-O-H, as azurite is metastable to it. Malachite ($Cu_2(OH)_2CO_3$) replaces the tenorite fields (Figs. 27 and 28), and forms from cuprite as indicated. Two contours for $a_c = 10^{-1}$ and 10^{-3} are shown in Fig. 29. The fields of CuS, Cu_2S, and native Cu are identical to those shown in Fig. 28.

Numerous diagrams for copper species have been published previously, including those by Garrels and Christ (1965), Anderson (1982), and others. If Fe is added to the Cu-C-S-O-H system, additional complexities arise, including phases such as chalcopyrite ($CuFeS_2$) and bornite (Cu_5FeS_4), and two Eh-pH diagrams for the system Cu-Fe-C-S-O-H are given in Garrels and Christ (1965; pp. 231, 232).

Table 25. Thermodynamic data for copper

Species (state)	ΔG_f^0 (kcal/gfw)	Reference
Cu (c)	0.00	Wagman et al. (1982)
Cu^+ (aq)	+11.94	Wagman et al. (1982)
Cu^{2+} (aq)	+15.65	Wagman et al. (1982)
Cu_2S (c)	−20.60	Wagman et al. (1982)
CuS (c)	−12.81	Wagman et al. (1982)
Cu_2O (c)	−34.98	Garrels and Christ (1965)
CuO (c)	−31.00	Wagman et al. (1982)
CuO_2^{2-} (aq)	−43.88	Wagman et al. (1982)
$Cu_2(CO_3)(OH)_2$ (c)	−213.58	Wagman et al. (1982)
$Cu_3(CO_3)_2(OH)_2$ (c)	−314.29	Wagman et al. (1982)

Abbreviations see Table 1

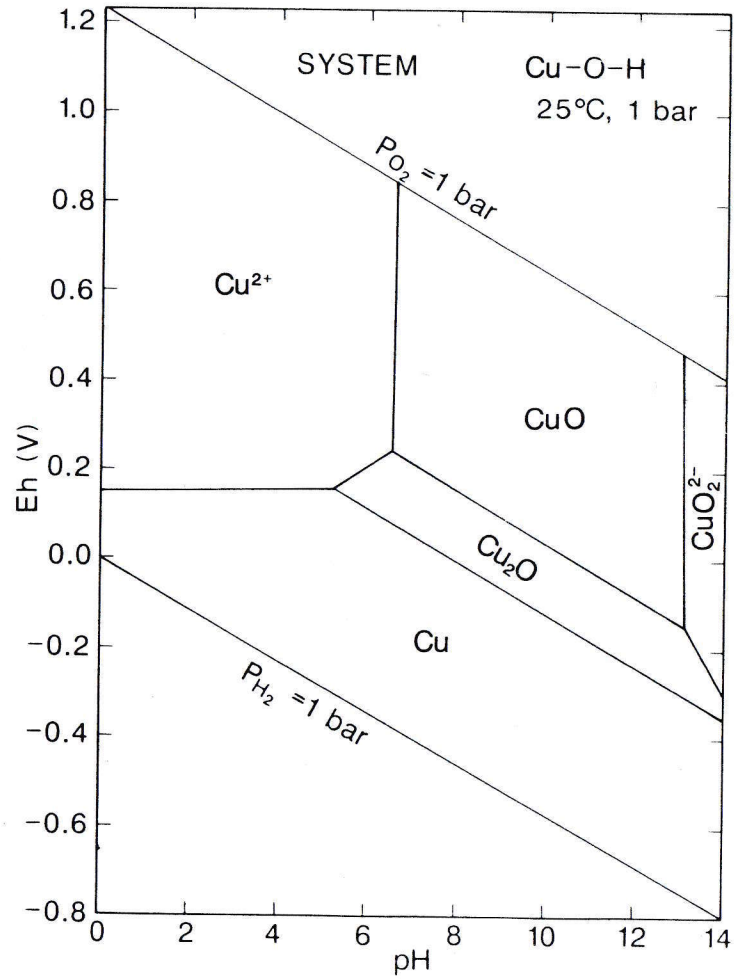

Fig. 27. Eh-pH diagram for part of the system Cu-O-H. The assumed activity for dissolved Cu = 10^{-6}. See text for discussion

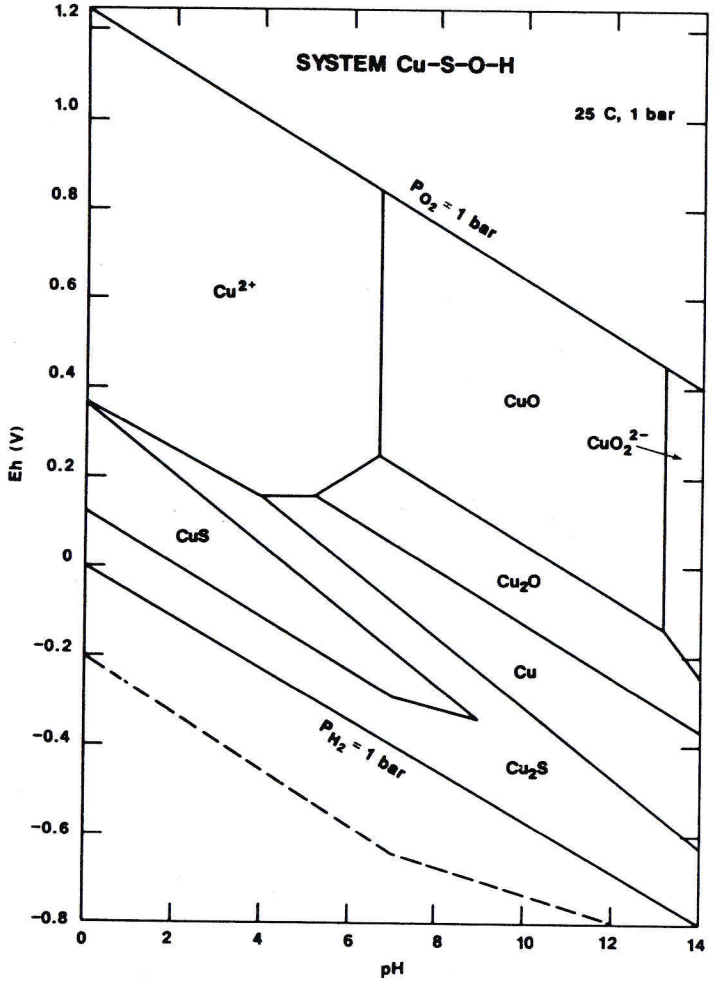

Fig. 28. Eh-pH diagram for part of the system Cu-S-O-H.
The assumed activities for dissolved species are: Cu = 10^{-6}, S = 10^{-3}.
See text for discussion

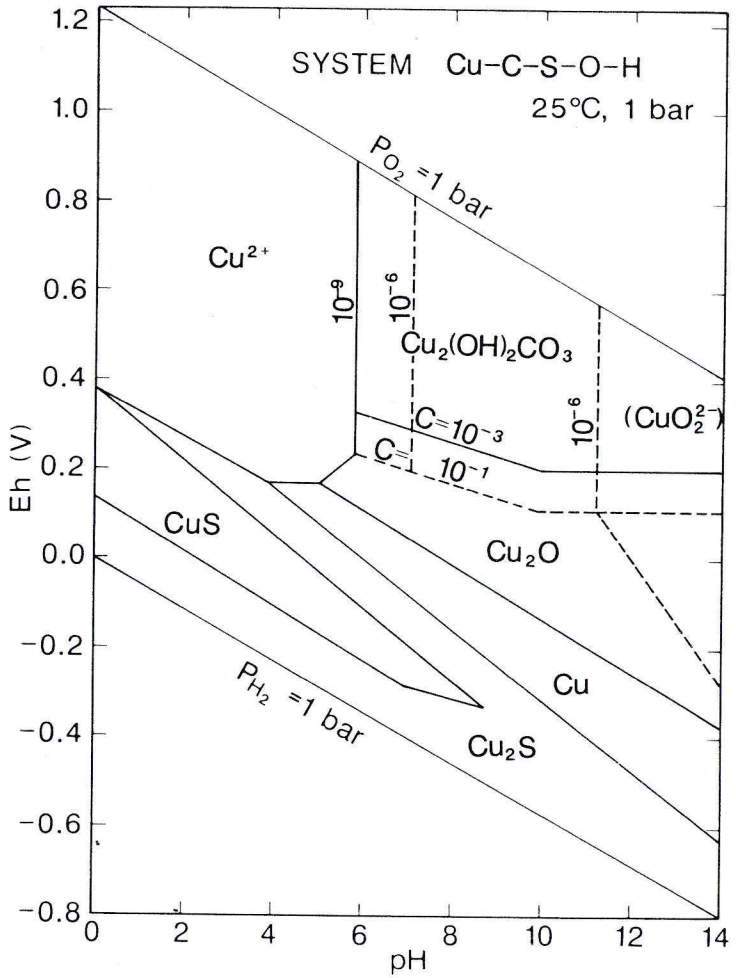

Fig. 29. Eh-pH diagram for part of the system Cu-C-S-O-H.
The assumed activities for dissolved species are: Cu = 10^{-6}, S = 10^{-3}, C = $10^{-1,-3}$
See text for discussion

SILVER

The Eh-pH diagram for silver species is shown in Fig. 30. The thermodynamic data for important silver species are given in Table 26.

The system Ag-S-O-H in Eh-pH space is dominated by a very large field of native silver. Under reducing conditions, Ag_2S (argenite) occupies a major part of the Eh-pH space as well. Note in Fig. 30 that native Ag can coexist with S(−II) and S(VI) aqueous species as a function of Eh. At high Eh, Ag oxidizes to Ag^+ or $Ag(OH)_2^-$ ($a_{Ag} = 10^{-8}$). When Cl is added to the system Ag-S-O-H, a field of $AgCl_2^-$ replaces much of the field for Ag^+ ($a_{Cl} = 10^{-3.5}$, showing the importance of dissolved Cl on Ag transport under oxidizing, acidic conditions.

Table 26. Thermodynamic data for silver

Species (state)	ΔG_f^0 (kcal/gfw)	Reference
Ag^{2+} (aq)	+64.29	Wagman et al. (1982)
Ag^+ (aq)	−18.43	Wagman et al. (1982)
Ag_2O (c)	−2.68	Wagman et al. (1982)
Ag_2O_2 (c)	+6.60	Wagman et al. (1982)
Ag_2O_3 (c)	+29.01	Wagman et al. (1982)
$Ag(OH)_2^-$ (aq)	−62.19	Wagman et al. (1982)
Ag_2S (c)	−9.72	Wagman et al. (1982)
$AgCl_2^-$ (aq)	−51.48	Wagman et al. (1982)

Abbreviations see Table 1

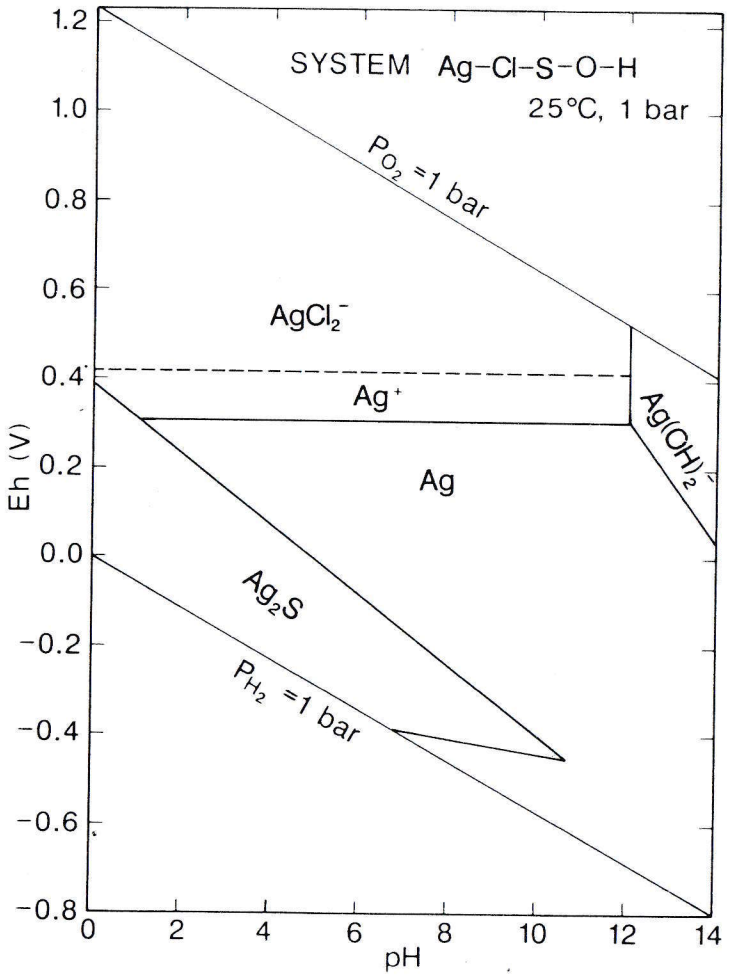

Fig. 30. Eh-pH diagram for part of the system Ag-Cl-S-O-H. The assumed activities for dissolved species are: Ag = 10^{-8}, S = 10^{-3}, Cl = $10^{-3.5}$. See text for discussion

GOLD

The Eh-pH diagrams for gold species are shown in Figs. 31 and 32. The thermodynamic data for important gold species are given in Table 27.

Gold species are shown in the Eh-pH space in Fig. 31, and, as expected, native gold occupies essentially all of the Eh-pH space. Yet this diagram, which intentionally includes dissolved Cl as well, illustrates that some gold transport is possible under very acidic, most oxidizing conditions ($a_{Cl} = 10^{-3.5}$). Further, increasing the activity of dissolved Cl will enlarge the fields for $AuCl_2^{4-}$ and $AuCl_2^-$. This is shown in Fig. 32, where $a_{Cl} = 10^{-1}$ coupled with $a_{Au} = 10^{-12}$ shows a large amount of Eh-pH occupied by Au-chloride complexes.

Further, gold transport may also occur by sulfide complexes (Garrels and Christ 1965).

Table 27. Thermodynamic data for gold

Species (state)	ΔG_f^0 (kcal/gfw)	Reference
Au^0 (c)	0.00	Wagman et al. (1982)
$Au(OH)_3$ (c)	−75.75	Wagman et al. (1982)
AuO_3^{3-} (aq)	−12.38	Wagman et al. (1982)
$HAuO_3^{2-}$ (aq)	−33.99	Wagman et al. (1982)
$H_2AuO_3^{1-}$ (aq)	−52.17	Wagman et al. (1982)
$AuCl_2^{1-}$ (aq)	−36.12	Wagman et al. (1982)
$AuCl_4^{1-}$ (aq)	−56.20	Wagman et al. (1982)
$HAuCl_4$ (aq)	−56.20	Wagman et al. (1982)
AuO_2 (c)	+48.00	Garrels and Christ (1965)
$Au(CN)_2^{1-}$ (aq)	−68.31	Wagman et al. (1982)
$Au(SCN)_2^{1-}$ (aq)	−60.21	Wagman et al. (1982)

Abbreviations see Table 1

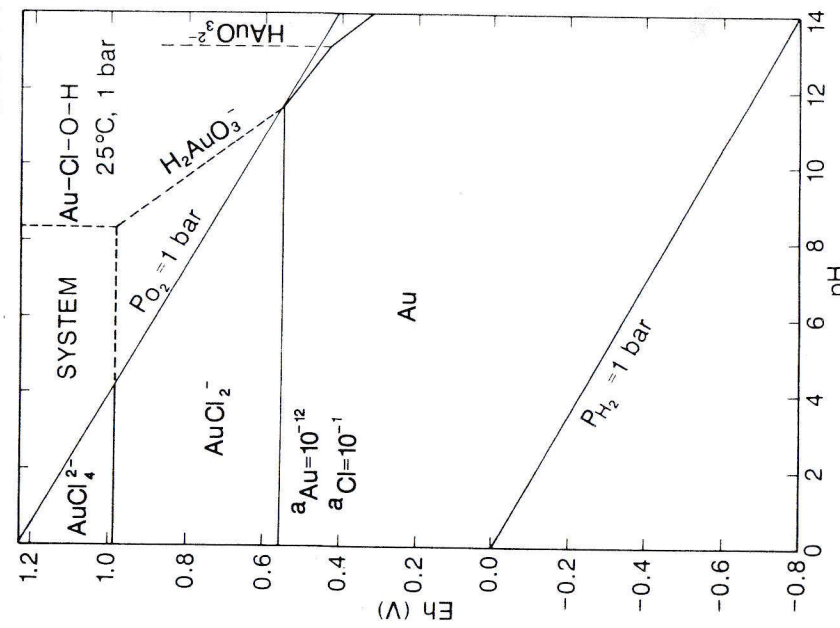

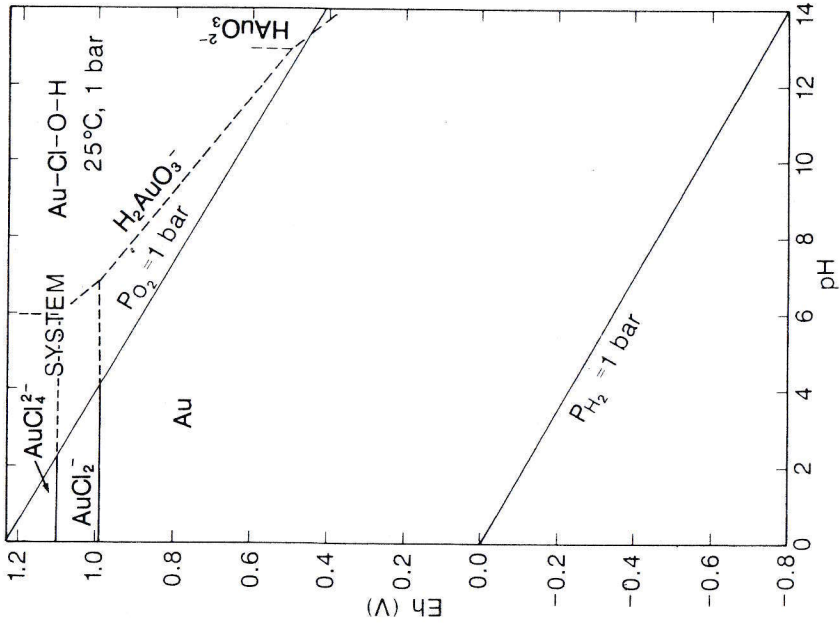

NICKEL

The Eh-pH diagrams for nickel species are shown in Figs. 33 and 34. The thermodynamic data for important nickel species are given in Table 28.

In the system Ni-O-H and for $a_{Ni} = 10^{-4}$ or 10^{-6} (Fig. 33), a fairly narrow field of $Ni(OH)_2$ (pH 8–12 or 9–11) separates a large field of Ni^{2+} from $HNiO_2^-$. Thus, nickel mobility in sulfur-poor systems under near-neutral to acidic conditions is obvious. The importance of S is shown in Fig. 34, where a large field of millerite (NiS) occurs below the sulfide-sulfate boundary ($a_S = 10^{-3}$). Not shown in Figs. 33 and 34 are the species $NiOH^+$ and $NiCO_3$, as both are metastable to Ni^{2+} and $Ni(OH)_2$, respectively. Unlike cobalt, nickel does not form a stable carbonate species.

Table 28. Thermodynamic data for nickel

Species (state)	ΔG_f^0 (kcal/gfw)	Reference
Ni^{2+} (aq)	−10.90	Wagman et al. (1982)
NiO (c)	−50.60	Wagman et al. (1982)
$Ni(OH)_2$ (c)	−106.88	Wagman et al. (1982)
NiS (c)	−19.00	Wagman et al. (1982)
$NiSO_4$ (c)	−181.57	Wagman et al. (1982)
$NiCO_3$ (c)	−146.39	Wagman et al. (1982)
$NiOH^+$ (c)	−54.40	Wagman et al. (1982)
$HNiO_2^-$ (aq)	−83.46	Garrels and Christ (1965)

Abbreviations see Table 1

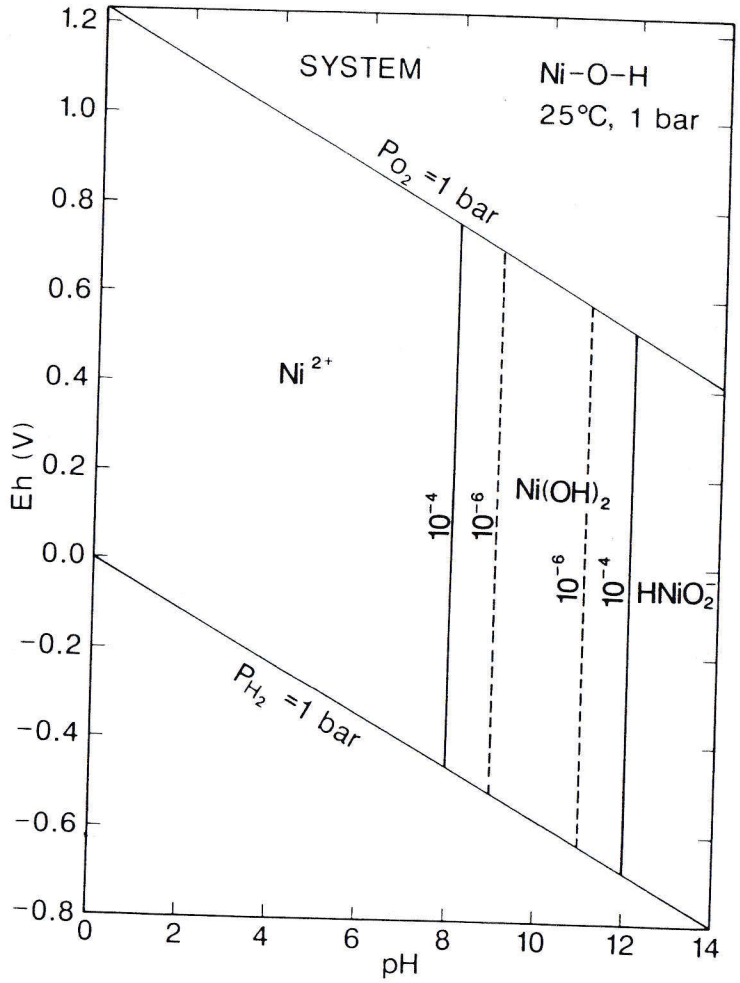

Fig. 33. Eh-pH diagram for part of the system Ni-O-H. Assumed activity of dissolved Ni = $10^{-4, -6}$. See text for discussion

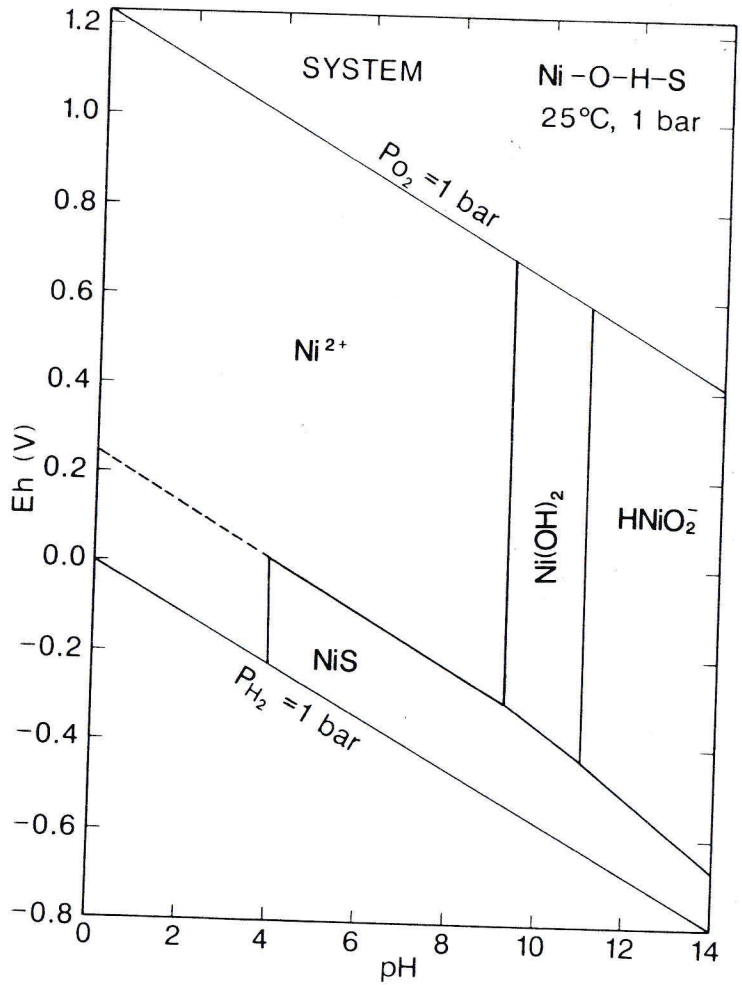

Fig. 34. Eh-pH diagram for part of the system Ni-O-H-S. Assumed activities for dissolved species are: Ni = $10^{-4,-6}$, S = 10^{-3}. See text for discussion

COBALT

The Eh-pH diagram for cobalt species is shown in Fig. 35. The thermodynar data for important cobalt species are given in Table 29.

Phase relations in the system Co-S-C-O-H are shown in Fig. 35 for following assumed activities: $a_{Co} = 10^{-6}$, $a_C = 10^{-3}$, $a_S = 10^{-3}$. Cobalt a nickel are often cited as a geochemical pair exhibiting near-ideal substituti for each other. This is indeed apparent in igneous rocks and in high tempe ture magmatic sulfides and in many metamorphic rocks. In the near-to-surfa environment, however, differences are apparent as illustrated by compari Fig. 35 for Co with Figs. 33 and 34 for Ni species. Cobalt possesses a Co(I valence, and a large field of Co_3O_4 occurs under oxidizing, neutral to ba pH (Fig. 35). In addition, cobalt forms a stable carbonate (spherocobalti $CoCO_3$), whereas nickel does not (cf. Figs. 33 and 34 with 35). Using old th modynamic data, Garrels and Christ (1965) have reported Eh-pH diagrams f Ni and Co species showing a stable field for Ni_3O_4 and $Co(OH)_3$, respective The data in Tables 28 (Ni) and 29 (Co) are better, however, and these speci do not appear in the water stability field. $Co(OH)_3$ oxidizing from Co_3 yields Eh = 1.76-0.059 pH, for example, well above the upper stability limit water. Data for Ni_3O_4 (Garrels and Christ 1965; see Fig. 7.29a, b, pp. 24 245) are not given. The boundary between $Ni(OH)_2$ and $Ni(OH)_3$, howeve yields Eh = 1.5-0.59 pH, again well above the upper stability limit of wate

Table 29. Thermodynamic data for cobalt

Species (state)	ΔG_f^0 (kcal/gfw)	Reference
Co^{2+} (aq)	−13.00	Wagman et al. (1982)
Co^{3+} (aq)	+32.03	Wagman et al. (1982)
CoO (c)	−51.20	Wagman et al. (1982)
Co_3O_4 (c)	−184.99	Wagman et al. (1982)
$HCoO_2^-$ (aq)	−82.97	Garrels and Christ (1965)
$Co(OH)_2$ (c)	−107.53	Wagman et al. (1982)
CoS (c)	−19.80	Garrels and Christ (1965)
$CoCO_3$ (c)	−155.57	Garrels and Christ (1965)
$Co(OH)_3$ (c)	−142.60	Garrels and Christ (1965)

Abbreviations see Table 1

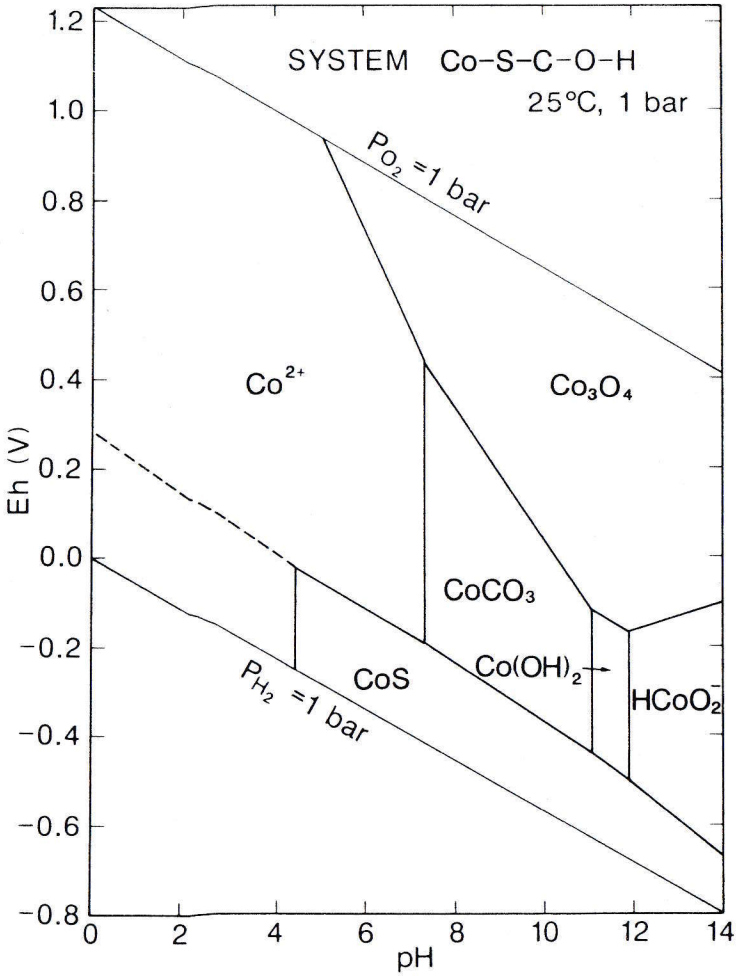

Fig. 35. Eh-pH diagram for part of the system Co-S-C-O-H. Assumed activities for dissolved species are: Co = 10^{-6}, C = 10^{-3}, S = 10^{-3}. See text for discussion

The Eh-pH diagrams for various iron species are given in Figs. 36 through 42 The thermodynamic data for important iron species are given in Table 30.

Several Eh-pH diagrams for the system Fe-(±C)-(±S)-O-H are presente here. Figure 36 shows the phase relations in the simple system Fe-O-H assum ing $Fe(OH)_3$ is the stable phase for the Fe(III) precipitate. Further, only Fe^{3+} is considered of the many Fe(III) aqueous species [$FeOH^{2+}$, $Fe(OH)_2^+$ $Fe_2(OH)_4^{2+}$, etc.], but this is justified since the total field of aqueous Fe(III species is in the small Eh-pH field shown in Fig. 36. The assumptio $a_{Fe} = 10^{-6}$ is also used. This figure is characterized by a large field o $Fe(OH)_3$, a large field of Fe^{2+}, and under reducing, basic conditions, a fiel of $Fe(OH)_2$. Magnetite is not considered in this diagram.

Addition of C to the simple Fe-O-H system is shown in Fig. 37. Here, small field of $FeCO_3$ appears in the pH range of 6.8 to 9.4, separating Fe^2 from $Fe(OH)_2$, and encroaching slightly on the $Fe(OH)_3$ field. Again magnetite is not assumed in this diagram.

The effect of adding Si to the system Fe-O-H, as the field of $Fe(OH)_2$ replaced by $FeSiO_3$, is shown in Fig. 38. $Fe(OH)_3$ is again considered as th stable Fe(III) phase, and magnetite is again assumed to be absent.

Figure 39 shows the phase relations in the system Fe-Si-O-H, now conside ing magnetite (Fe II, III) as well as Fe(II) and Fe(III) phases. With Fe(OH again chosen as the stable Fe(III) phase, a very large magnetite field appear Klein and Bricker (1977) have used a similar diagram to comment on the origi of banded iron formations. The $FeSiO_3$ field replaces the $Fe(OH)_2$ field Fig. 36. To a first approximation, the $FeSiO_3$ field can be assumed to be clo to that for Fe(II) silicates found in banded iron formations.

Another version of the Fe-O-H-Si system (Fig. 40) considers FeO·O (goethite) as the stable Fe(III) phase. Magnetite still exists, separating FeSi from goethite, but its Eh-pH stability field is much smaller than wh $Fe(OH)_3$ is considered (Fig. 39).

Addition of C to the Fe-Si-O-H system with FeO·OH as the stable Fe(II phase is shown in Fig. 41, with, similar to Fig. 37, the siderite field separati Fe^{2+} from both Fe_3O_4 and $FeSiO_3$, and encroaching slightly into the FeO·O field.

Finally, the effect of sulfur on the Fe-O-H system is considered in Fig. 4 Here, the reducing conditions below the sulfide-sulfate boundary yield a lar field of pyrite which, along with the very small pyrrhotite field (at highest p and most reducing conditions), obliterates most of the magnetite field and the $FeSiO_3$ [or $Fe(OH)_2$] field, and also the field of $FeCO_3$. Hematite (Fe_2O is shown as the stable Fe(III) phase, since both $Fe(OH)_3$ and FeO·OH will a

to Fe_2O_3 (although the kinetics for this aging may be very slow). Figure 42 is the standard reference diagram for Fe species. Garrels and Christ (1965) and Drever (1982) have presented numerous diagrams for Fe systematics, and the reader is referred to their work for more detail. They point out, for example, that even when S activity is greatly reduced (to near 10^{-6}), a small field of pyrite still exists in the neutral pH range along the sulfide-sulfate boundary, demonstrating its widespread occurrence over widely differing chemical conditions.

Other Fe Eh-pH diagrams have been given by Hem (1977) and more recently by Winters and Buckley (1986) who advocate consideration of aqueous $FeSi_3O_3(OH)_8^0$ as an important species.

Table 30. Thermodynamic data for iron

Species (state)	ΔG_f^0 (kcal/gfw)	Reference
Fe^{2+} (aq)	−18.86	Wagman et al. (1982)
Fe^{3+} (aq)	−1.12	Wagman et al. (1982)
FeO_2^{2-} (aq)	−70.58	Wagman et al. (1982)
Fe_2O_3 (c)	−177.39	Wagman et al. (1982)
Fe_3O_4 (c)	−242.69	Wagman et al. (1982)
$Fe(OH)_3$ (c)	−166.47	Wagman et al. (1982)
$Fe(OH)_2$ (c)	−116.30	Winters and Buckley (1986)
FeO·OH (c)	−116.77	Robie et al. (1978)
FeS_2 (c)	−39.89	Wagman et al. (1982)
FeS (c)	−24.00	Wagman et al. (1982)
$FeSiO_3$ (c)	−267.16	Winters and Buckley (1986)
$FeCO_3$ (c)	−159.34	Winters and Buckley (1986)
$FeSi_3O_3(OH)_8^0$ (aq)	−898.00	Winters and Buckley (1986)

Abbreviations see Table 1

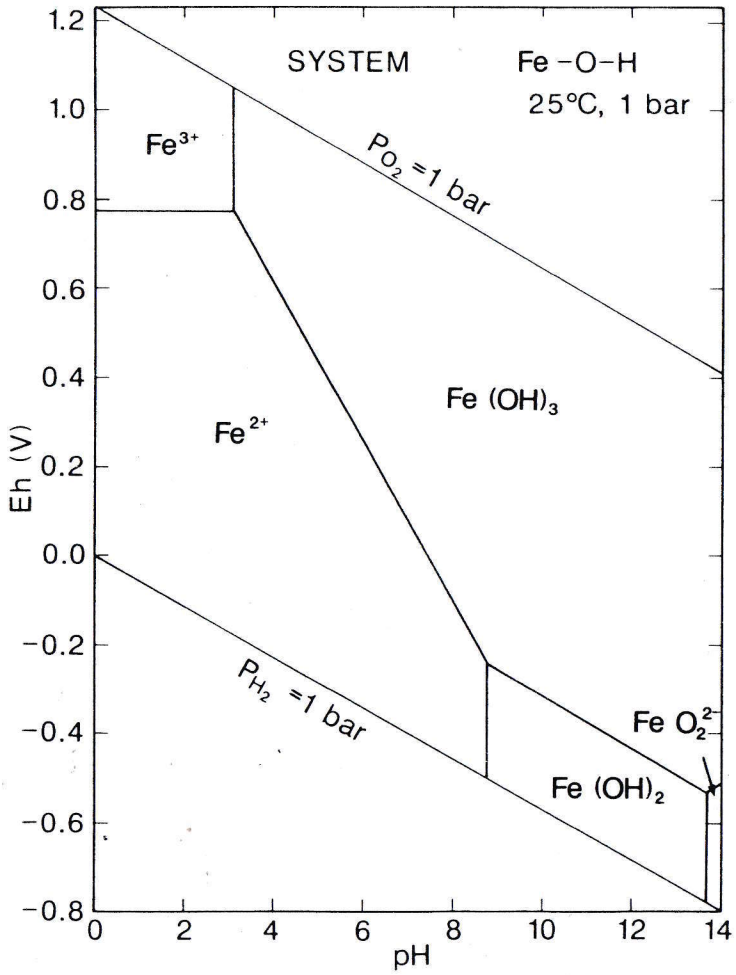

Fig. 36. Eh-pH diagram for part of the system Fe-O-H assuming $Fe(OH)_3$ as stable Fe(III) phase. Assumed activity of dissolved Fe = 10^{-6}. See text for discussion

PLATINUM

The Eh-pH diagram for platinum species is shown in Fig. 46. The thermodynamic data for important platinum species are given in Table 34.

Platinum species present in the terrestrial environment include native platinum, platinum oxide-hydroxide, and platinum sulfides. Under the sulfide-sulfate boundary, PtS (cooperite) and PtS_2 occur as shown. As in the case of several other metals (i.e., mercury, silver, copper, other platinoids), when sulfide is oxidized to sulfate, the metal ion in the sulfides is reduced as a counterbalancing attempt to the oxidation. The field of native Pt in the Eh-pH diagram is immense. At high Eh Pt(0) oxidizes to $Pt(OH)_2$ and then to PtO_2 near the upper stability limit of water. A small field of Pt^{2+} occures under extreme acidic and highly oxidizing conditions.

Previous diagrams for Pt include those by Pourbaix (1966) for metal-water systems, and by Westland (1981) and Brookins (1987b) for metal-water-sulfur systems. These diagrams are close to each other and to the one presented here, although Westland (1981) uses $PtO \cdot xH_2O$ instead of $Pt(OH)_2$ and $PtO_2 \cdot xH_2O$ instead of PtO_2.

Table 34. Thermodynamic data for platinum

Species (state)	ΔG_f^0 (kcal/gfw)	Reference
PtS (c)	−21.6	Latimer (1952)
PtS_2 (c)	−25.6	Latimer (1952)
$Pt(OH)_2$ (c)	−68.2	Latimer (1952)
PtO_2 (c)	−20.0	Pourbaix (1966)
Pt^{2+} (aq)	+54.8	Pourbaix (1966)

Abbreviations see Table 1

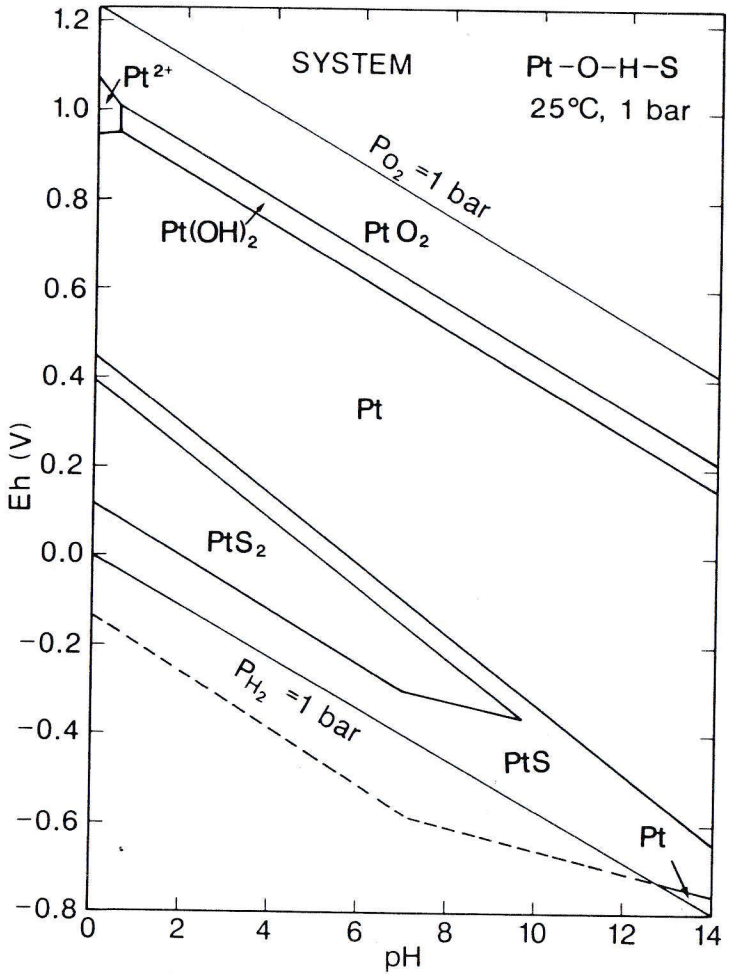

Fig. 46. Eh-pH diagram for part of the system Pt-O-H-S. Assumed activities for dissolved species are: Pt = 10^{-8}, S = 10^{-3}. See text for discussion

MANGANESE

The Eh-pH diagrams for manganese species are shown in Figs. 49 and 50. The thermodynamic data for important manganese species are given in Table 37.

Figure 49 shows the Eh-pH phase relations in the system Mn-O-H. Much of the field is occupied by Mn^{2+}, and the oxides and oxyhydroxides of Mn become important only under basic pH except at high Eh. Under surface to near-surface weathering conditions, various MnO_2 polymorphs (pyrolusite, todorokite, etc.) form. The MnO_2 field is important as it explains the abundance of Mn-oxide stains and dendrites on weathered surfaces.

Figure 50 shows the effect of adding both S and C to the Mn-O-H system. The assumed activities are 10^{-3} for both dissolved S and C, and 10^{-6} for dissolved Mn. The field of $MnCO_3$ (rhodochrosite) is important as Mn in $MnCO_3$ can be fixed with cogenetic sulfides or just above the sulfide-sulfate boundary. The field of MnS (alabandite) is very small, attesting to the rarity of MnS in nature. Manganese compounds are often quite impure, containing iron and other elements.

Previous Eh-pH diagrams for Mn species include Garrels and Christ (1965) and Hem (1981).

Table 37. Thermodynamic data for manganese

Species (state)	ΔG_f^0 (kcal/gfw)	Reference
Mn^{2+} (aq)	−54.52	Wagman et al. (1982)
MnO (c)	−86.74	Wagman et al. (1982)
MnO_2 (c)	−111.17	Wagman et al. (1982)
Mn_2O_3 (c)	−210.59	Wagman et al. (1982)
Mn_3O_4 (c)	−306.69	Wagman et al. (1982)
$MnOH^+$ (aq)	−96.80	Wagman et al. (1982)
$Mn(OH)_2$ (c)	−146.99	Wagman et al. (1982)
$Mn(OH)_3^-$ (aq)	−177.87	Wagman et al. (1982)
MnS (c)	−52.20	Wagman et al. (1982)
$MnCO_3$ (c)	−195.20	Wagman et al. (1982)

Abbreviations see Table 1

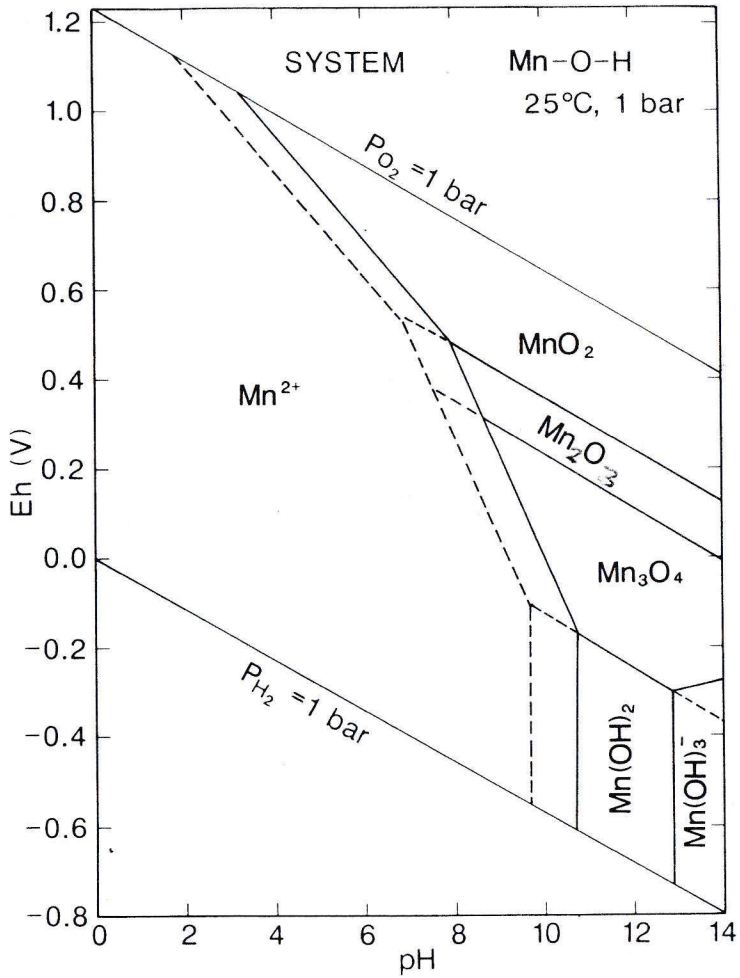

Fig. 49. Eh-pH diagram for part of the system Mn-O-H. Assumed activity for Mn = 10^{-6}. See text for discussion

CHROMIUM

The Eh-pH diagram for chromium species is shown in Fig. 55. The thermodynamic data for important chromium species are given in Table 40.

Much of the Eh-pH space (Fig. 55) is occupied by insoluble Cr_2O_3. This species dissolves to form $CrOH^{2+}$ slightly below pH = 5 (Cr activity = 10^{-6}), and to form CrO_2^- above pH 13.5. Cr(III) oxidizes to form Cr(VI) as $HCrO_4^-$ and CrO_4^{2-} ions at high Eh. Cr(VI) species are known carcinogens, and it is noted that both $HCrO_4^-$ and CrO_4^{2-} occupy fairly large Eh-pH fields. Various chromates are known in nature (crocoite, etc.). Cr_2O_3 is rare in nature as most Cr(III) is incorporated into chromites or other chromian spinels.

Table 40. Thermodynamic data for chromium

Species (state)	ΔG_f^0 (kcal/gfw)	Reference
Cr^{3+} (aq)	−51.50	Barner and Scheuerman (1978)
Cr_2O_3 (c)	−252.89	Wagman et al. (1982)
$Cr(OH)^{2+}$ (aq)	−103.00	Latimer (1952)
$Cr(OH)_2^+$ (aq)	−151.20	Garrels and Christ (1965)
CrO_2^- (aq)	−128.00	Garrels and Christ (1965)
CrO_4^{2-} (aq)	−173.94	Wagman et al. (1982)
$HCrO_4^-$ (aq)	−182.77	Wagman et al. (1982)
$Cr_2O_7^{2-}$ (aq)	−310.97	Wagman et al. (1982)

Abbreviations see Table 1

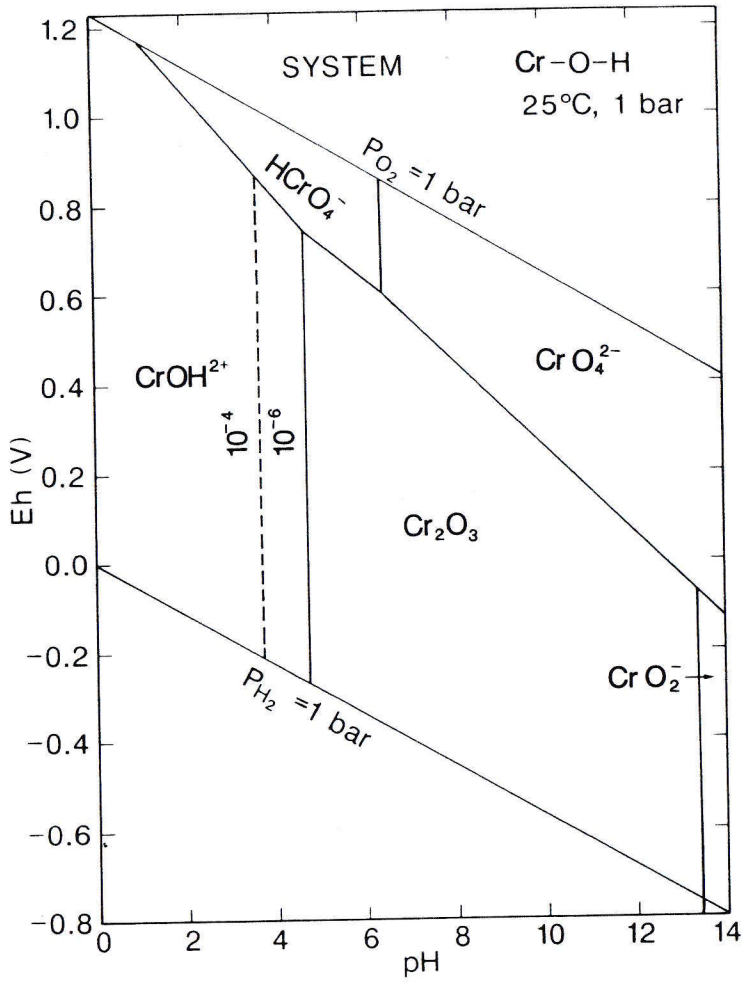

Fig. 55. Eh-pH diagram for part of the system Cr-O-H. Assumed activity of dissolved Cr = 10^{-6}. See text for discussion

MOLYBDENUM

The Eh-pH diagram for molybdenum species is shown in Fig. 56. The thermodynamic data for important molybdenum species are given in Table 41.

Important phases in the system Mo-S-O-H are shown in Fig. 56. The species MoS_2 occupies the sulfide-stable part of the diagram, and aqueous species dominate under sulfate-stable conditions, except for a small field of ilsemannite (Mo_3O_8). Mo species in natural waters under oxidizing conditions occur as various Mo(V, VI) oxyions. It is transported with similar ions, i.e., U, Se, V, As oxyions, and, when chemically reducing conditions are encountered, these various oxyions are replaced by insoluble, lower valence compounds. Thus, Mo is incorporated into the cryptocrystalline variety of molybdenite called jordisite (Brookins 1977). Similarly, the other ions yield separate compounds of other elements, i.e., U in pitchblende or coffinite, Se in native Se or in $Fe(S,Se)_2$, V in oxides or clay minerals, and As in sulfides. If subsequent oxidation encroaches on this group of compounds, then they tend to be segregated. Mo may be enriched by such a secondary process or, alternately, may be distributed but still enriched over background, thus making it an useful metal for geochemical U prospecting.

Molybdenum is a known toxin, and responsible for fairly widespread disease among cattle. Because Mo is enriched in uranium ores, some Mo separated from the ore during the milling process accumulates on the mill tailings piles area. As shown in Fig. 56, Mo is very soluble under high Eh conditions, and can migrate easily in the presence of water. Hence, mill tailings piles must be carefully monitored to ensure against Mo loss.

Table 41. Thermodynamic data for molybdenum

Species (state)	ΔG_f^0 (kcal/gfw)	Reference
$HMoO_4^-$ (aq)	−213.60	Garrels and Christ (1965)
MoO_4^{2-} (aq)	−199.88	Wagman et al. (1982)
MoS_2 (c)	−53.99	Wagman et al. (1982)
Mo_3O_8 (c)	−480.00	Titley and Anthony (1961)
MoO_2^+ (aq)	−122.80	Gerasimov et al. (1963)
MoO_2 (c)	−127.39	Wagman et al. (1982)
MoO_3 (c)	−159.65	Wagman et al. (1982)

Abbreviations see Table 1

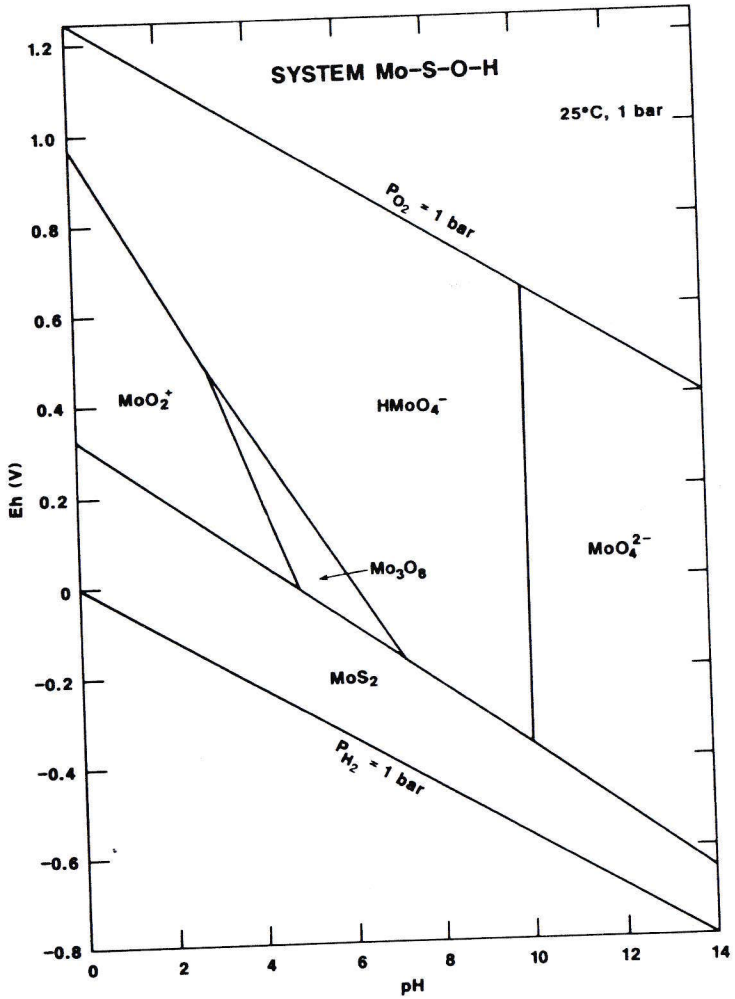

Fig. 56. Eh-pH diagram for part of the system Mo-S-O-H. Assumed activities for dissolved species are: Mo = 10^{-8}, S = 10^{-3}. See text for discussion

TANTALUM

The Eh-pH diagram for tantalum species is shown in Fig. 60. The thermodynamic data for important tantalum species are given in Table 45.

Like Nb, only Ta(V) is important in nature. However, unlike Nb, in the system Ta-O-H a moderate field of TaO_2^+ occurs below pH = 5. Ta_2O_5 is stable over all Eh at higher pH. While most Ta is contained in tantalate-niobate salts, weathering under mildly to more pronounced acidic conditions may release Ta(V) as TaO_2^+.

Table 45. Thermodynamic data for tantalum

Species (state)	ΔG_f^0 (kcal/gfw)	Reference
TaO_2^+ (aq)	−201.39	Wagman et al. (1982)
Ta_2O_5 (c)	−456.79	Wagman et al. (1982)

Abbreviations see Table 1

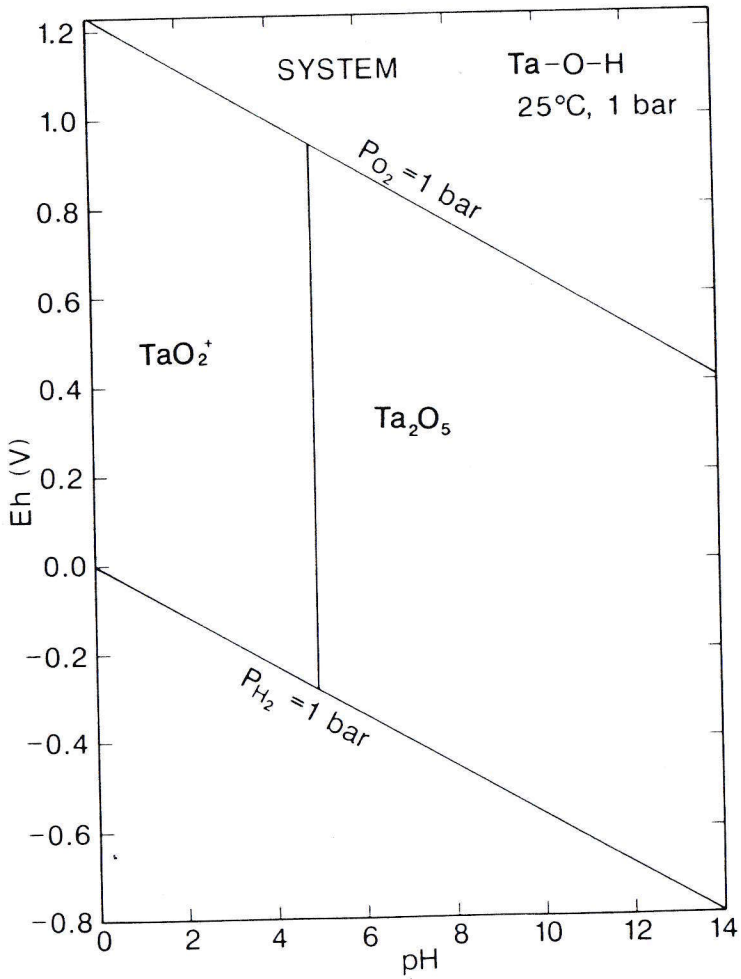

Fig. 60. Eh-pH diagram for part of the system Ta-O-H. Assumed activity of dissolved Ta = 10^{-8}. See text for discussion

PLUTONIUM

The Eh-pH diagrams for plutonium species are shown in Figs. 82 and 83. The thermodynamic data for important plutonium species are given in Table 52.

The most commonly produced Eh-pH diagram for plutonium species is shown in Fig. 82 for the system Pu-(C)-O-H. Most of the stability field of water is covered by PuO_2, with subordinate fields of Pu^{3+} and very small fields of Pu^{4+}, PuO_2^+, and $Pu(OH)_5^-$. The Pu-carbonate complex, $PuO_2(OH)_2CO_3^{2-}$, plots above the upper stability limit for water (assuming activities of: $a_{Pu} = 10^{-8}$, $a_C = 10^{-3}$). This large stability field of PuO_2 attests to the extreme immobility of Pu in nature, such as at the Oklo Natural Reactor, Gabon (Brookins 1984). Further, activity of dissolved Pu must be lowered to unrealistic levels before there is an appreciable diminishing of the PuO_2 field.

In Fig. 83, however, in the system Pu-O-H-C, if $Pu(OH)_4$ is chosen as the preferred Pu(IV) solid, the diagram is strikingly different. Here, the solids $Pu(OH)_4$ and $Pu_2(CO_3)_3$ are subordinate to Pu^{3+} and $Pu(OH)_5^-$. The fields of Pu^{4+} and PuO_2^+ remain small. The importance of this diagram is that under high water to rock ratios, Pu may be mobile if $Pu(OH)_4$ is formed instead of PuO_2. It must be emphasized, however, that $Pu(OH)_4$ will age quickly to PuO_2 in most natural settings.

Previously published Eh-pH diagrams for Pu species include those by the author (Brookins 1978b, c, 1984), Lemire and Tremain (1980), and Krauskopf (1986). The data of Table 52 are preferred over data used in these earlier studies, however; hence, Figs. 82 and 83 should be referenced hereon.

Table 52. Thermodynamic data for plutonium

Species (state)	ΔG_f^0 (kcal/gfw)	Reference
Pu^{3+} (aq)	−138.15	OECD (1985)
Pu^{4+} (aq)	−114.96	OECD (1985)
Pu_2S_3 (c)	−233.99	OECD (1985)
PuO_2 (c)	−238.53	OECD (1985)
$Pu(OH)_5^{1-}$ (aq)	−378.10	OECD (1985)
PuO_2^{1+} (aq)	−203.10	OECD (1985)
$PuO_2(OH)_2CO_3^{2-}$ (aq)	−413.99	OECD (1985)
$Pu(OH)_4$ (c)	−340.82	OECD (1985)
$Pu_2(CO_3)_3$ (c)	−697.44	OECD (1985)

Abbreviations see Table 1

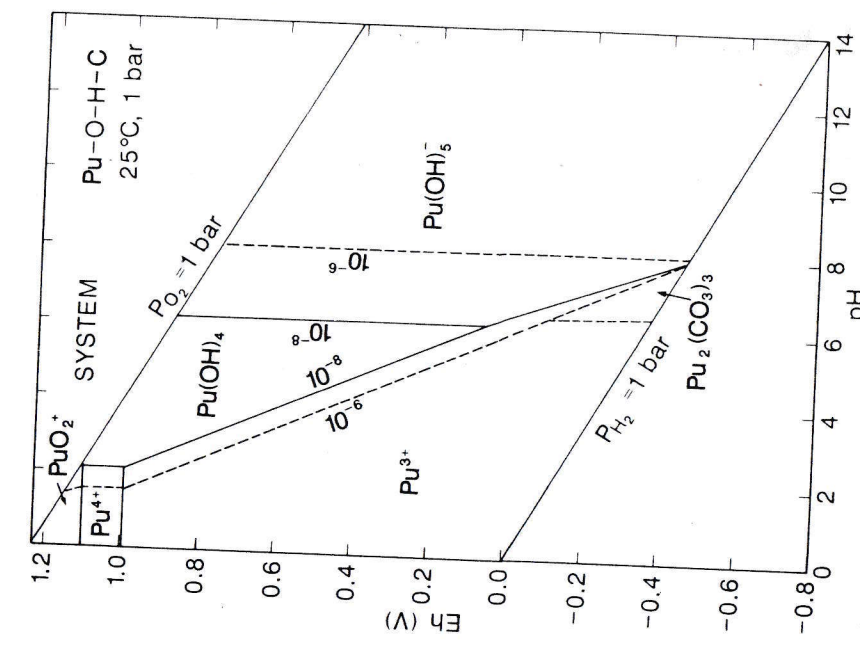

Fig. 83. Eh-pH diagram for part of the system Pu-O-H-C. Assumed activities for dissolved species are: $Pu = 10^{-8}$, $C = 10^{-3}$. $Pu(PH)_4$ is chosen as the Pu(IV) oxide solid

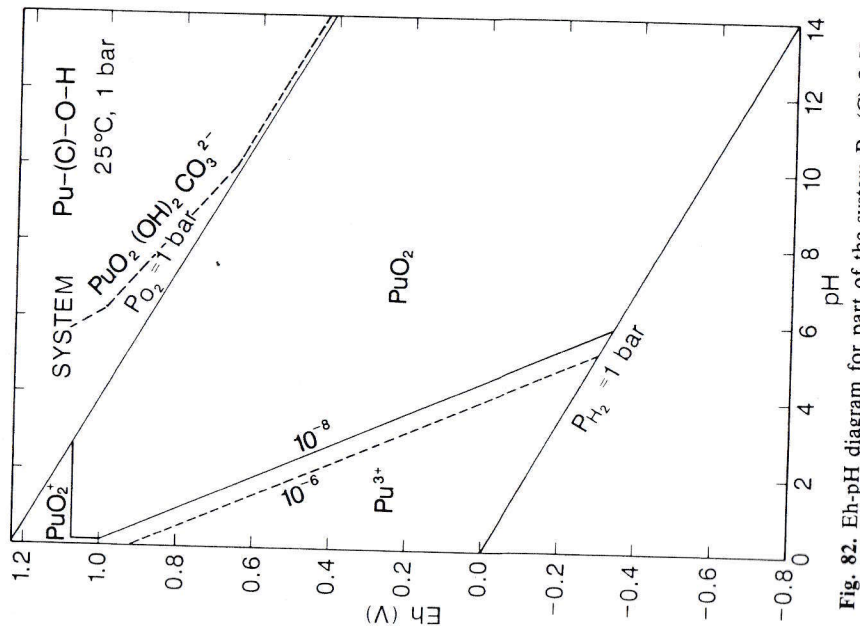

Fig. 82. Eh-pH diagram for part of the system Pu-(C)-O-H. Assumed activities for dissolved species are: $Pu = 10^{-8}$, $C = 10^{-3}$. See text for discussion

Finally, in the absence of dissolved C, coffinite shows a stability field below pH = 7. Hence, coffinite would not be expected in the hematite-pitchblende high-grade sedimentary ores, and this is consistent with observation. Similarly, under acidic reducing conditions and in carbonate-poor environments, coffinite may form.

Numerous Eh-pH diagrams for U species are present in the literature. In addition to the author's previous efforts (Brookins 1976a, 1977, 1978b, 1979a, c, 1982, 1984), there are those presented by Garrels (1959), Garrels and Christ (1965), Langmuir (1978), and Lemire and Tremain (1980). The reader is referred to these sources for more detail. Not covered in Figs. 87–91 are the several U(VI) solid species; these have been discussed by Garrels and Christ (1965), Brookins (1981), and in great depth by Tripathi (1984).

Table 54. Thermodynamic data for uranium

Species (state)	ΔG_f^0 (kcal/gfw)	Reference
UO_2 (c)	−246.62	OECD (1985)
$U(OH)_5^{1-}$ (aq)	−389.77	OECD (1985)
U_3O_8 (c)	−805.35	OECD (1985)
UO_2^{2+} (aq)	−227.66	OECD (1985)
UO_2CO_3 (c)	−373.50	OECD (1985)
UO_2CO_3 (aq)	−367.57	OECD (1985)
$UO_2(CO_3)_2^{2-}$ (aq)	−502.97	OECD (1985)
$UO_2(CO_3)_3^{4-}$ (aq)	−635.57	OECD (1985)
$USiO_4$ (c)	−445.00	Langmuir (1978)

Abbreviations see Table 1

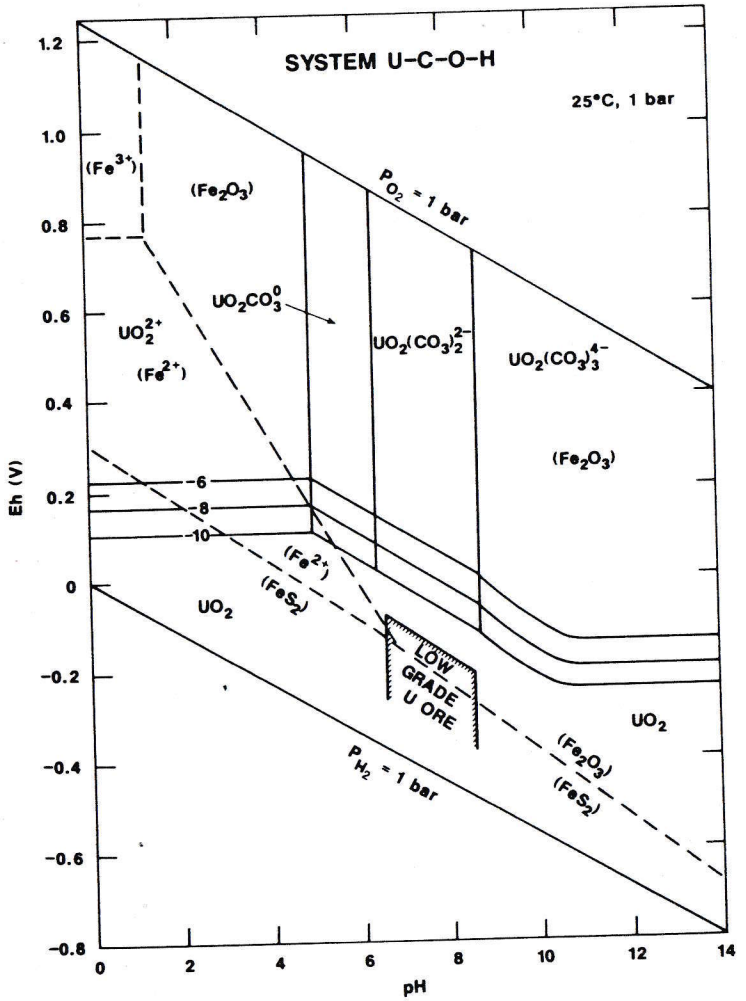

Fig. 87. Eh-pH diagram for part of the system U-C-O-H with part of the system Fe-S-O-H superimposed.
Assumed activities for dissolved species are: $U = 10^{-6, -8, -10}$, $C = 10^{-3}$, $Fe = 10^{-6}$, $S = 10^{-3}$. Area marked *U Ore* from Brookins (1982). See text for details